Asset Diversification versus Climate Action

Christoph Hambel[a] Holger Kraft[b] Frederick van der Ploeg[c]

Current version: March 23, 2022

Abstract: Asset pricing and climate policy are analyzed in a global economy where consumption goods are produced by both a green and a carbon-intensive sector. We allow for two types of damages from global warming. Given that the economy is initially heavily dependent on carbon-intensive capital, the desire to diversify assets complements the attempt to mitigate economic damages from climate change. In the longer run, however, a trade-off between diversification and climate action emerges. We derive the optimal carbon price, the equilibrium risk-free rate, and risk premia. Climate disasters, which are more likely to occur sooner as temperature rises, significantly increase risk premia on financial assets.

Keywords: decarbonization, diversification, carbon price, asset prices, green assets, disaster risk

JEL subject codes: D81, G01, G12, Q5, Q54

[a] Faculty of Economics and Business, Goethe University, Theodor-W.-Adorno-Platz 3, 60323 Frankfurt am Main, Germany. Phone: +49 (0) 69 798 33687.
E-mail: christoph.hambel@finance.uni-frankfurt.de

[b] Faculty of Economics and Business, Goethe University, Theodor-W.-Adorno-Platz 3, 60323 Frankfurt am Main, Germany. Phone: +49 (0) 69 798 33699.
E-mail: holgerkraft@finance.uni-frankfurt.de

[c] University of Oxford, Department of Economics, OXCARRE, Manor Road Building, Oxford OX1 3UQ, U.K. Phone: +44 (0) 1865 281285.
E-mail: rick.vanderploeg@economics.ox.ac.uk. Also affiliated with ASE, University of Amsterdam, P.O. Box 15551, 1001 NB Amsterdam, the Netherlands, and CEPR.

We thank Daniel Andrei, Patrick Bolton, Julia Braun, Ruediger Kiesel, Thomas Lontzek, Colin Mayer, Stavros Panageas, Armon Rezai, Eduardo Schwartz, Christian Traeger, Frank Venmans, and the participants of the Finance seminar at McGill, seminars at Humboldt University, the University of Lausanne, the Bundesbank and de Nederlandsche Bank, the European Finance Association (EFA) Meeting 2020, the European Economics Association (EEA) Meeting 2020, the SURED Meeting 2020, the EAERE Meeting 2020, the EBI Global Annual Conference 2020, the German Finance Association Meeting 2021, and the Verein fuer Socialpolitik (VfS) Meeting 2021 for helpful comments and suggestions. All remaining errors are our own. Christoph Hambel and Holger Kraft gratefully acknowledge financial support by the Deutsche Forschungsgemeinschaft (DFG).

1 Introduction

Climate change impacts all areas of human life and impacts economic activity.[1] To avoid carbon-dioxide emissions and climate change, emissions-free technologies and renewable energies are developed. Depending on the perceived severity of the consequences of climate change, there are different opinions about how urgent it is to transition to a less carbon-intensive or carbon-free economy. We are interested in the interplay between financial considerations and policies to mitigate climate change and answer two key policy questions. First, does the financial need to diversify assets hamper or help the fight against climate policy and how does it affect optimal carbon pricing? Second, how does climate change and the desire to combat it affects the pricing of green and dirty assets? We highlight that there is a subtle dynamic interdependence between the financial goal to diversify assets in portfolios and the environmental goal to reduce carbon emissions.

Our economic framework is a stochastic macroeconomic growth model with two capital stocks and two energy sources. The green sector takes carbon-free or green energy as input. The dirty sector is carbon-intensive and requires fossil fuel whose combustion leads to carbon emissions. Although our contribution is more methodological than empirical, the dirty carbon sector would include coal-fired power stations, steel, cement, aluminium, fossil-based transport (including the sea and airports), and the oil, gas and coal sectors. The green sector includes the sectors that do not depend excessively on oil, gas or coal but depend on solar or wind energy.

There are two types of capital stocks, dirty and green. Investments and capital reallocation from the dirty to the green capital stock are both subject to adjustment costs. Capital stock accumulation is exposed to diffusive shocks as well as the risk of macroeconomic disasters. We have a two-sector endogenous growth (AK) model and abstract from directed technical change towards green technologies (cf. Bovenberg and Smulders 1996; Acemoglu et al. 2012). Emissions are proportional to fossil fuel use and temperature is driven by cumulative emissions.[2]

We allow for two potential channels for the effect of climate change on economic activity: higher temperature leads to a higher share of damages in pre-damage output as in the seminal DICE-2016R2 model (e.g., Nordhaus 2017). Additionally, higher temperatures increase the Poisson risk of climate-related disasters (cf. Bansal et al. 2019; Karydas and Xepapadeas 2019).

We first establish the interplay between the intensity of climate action proxied by the carbon price and the economic motive to diversify. Given that the economy is initially dominated by the carbon-intensive

[1] See, e.g., Scheffers et al. (2019).

[2] See Matthews et al. (2009), Allen et al. (2009), IPCC (2014), van der Ploeg (2018), and Dietz and Venmans (2019), among others, for further references.

capital stock, there are two complementary goals. The first one is to mitigate climate change by decarbonizing the economy. The second goal is to diversify the economy. Both goals require decision makers to initially reduce the dirty capital stock. The speed of transition towards a low-carbon economy is thus initially amplified by the diversification motive. Over time, however, the two goals start to conflict. From a diversification perspective, the process should be stopped if there is a balance between green and dirty capital. But from an environmental perspective the dirty capital stock should eventually be run down completely. Our various calibrations show, however, that this does not occur unless damages from global warming are extremely severe relative to those in the DICE model of Nordhaus (2017). Effectively, climate policy drives the dirty capital stock below the fully diversified level, but diversification considerations may prevent policymakers from driving it to zero.

Second, we investigate the interplay between climate change and pricing of green and dirty assets. We analyze the dynamics of the risk-free rate and risk premia during the transition from a carbon-intensive towards a low- or zero-emissions economy. To separate economic from climate effects, our model includes the risk of macroeconomic disaster shocks as in Barro (2006, 2009) and Pindyck and Wang (2013). Therefore, our model can generate the high equity premium and low risk-free rate observed in historical data even when climate change has no significant impact on the economy. Taking the effects of climate change into account, we find that the risk-free interest rate decreases in response to rising temperatures reflecting the additional precautionary savings needed to cope with global warming. However, risk premia are only significantly affected if we allow for potential climate disasters for which the probability of them occurring increases with temperature. Then, the risk premia increase with higher temperature. Without such temperature-dependent disasters, this effect is modest.

We enrich a well-known asset pricing framework with rare macroeconomic disasters as in Barro (2006, 2009) or Wachter (2013) by adding the climate module of an integrated assessment model (IAM). Our representative agent has recursive utility as in Bansal and Yaron (2004) and Pindyck and Wang (2013). If the size of the two sectors is exogenous and the effect of climate change is disregarded, the two-tree model analyzed in Cochrane et al. (2007) arises as a special case.

The climate component is inspired by IAMs which typically have only one sector and do not focus on asset pricing. For example, the DICE model has one sector and is widely used to study optimal carbon abatement and carbon pricing. It combines a Ramsey-type model for capital allocation with deterministic dynamics of the economy, emissions, carbon dioxide and global temperature (e.g., Nordhaus 1992, 2017). In frameworks with recursive utility, Crost and Traeger (2014), Jensen and Traeger (2014), Ackerman et al. (2013), Bretschger and Vinogradova (2019), van den Bremer and van der Ploeg (2021), Hambel et al. (2021a), Lemoine (2021) analyze stochastic models of the economy and the climate. Cai

and Lontzek (2019) extend the DICE model with stochastic growth and the risk of tipping points. Furthermore, there are IAMs that do not fall into the class of DICE models. For instance, Golosov et al. (2014) obtain closed-form solutions in a framework with log utility, Cobb-Douglas production, full depreciation in one discrete time period, and damages that are an exponential function of the atmospheric carbon stock. Traeger (2019) generalizes this setting to recursive preferences and provides a description of the carbon cycle and the climate system. He also allows for epistemological uncertainty and anticipated learning.

Few papers combine asset pricing with an IAM. Barnett et al. (2020) analyze a stochastic one-sector macroeconomic DSGE model with stochastic economic growth rates and endogenous investments in fossil fuel reserves. They also address preference-based concerns about ambiguity and model misspecification. Barnett (2020) uses an extended Fama-French 3-factor model to estimate negative effects of temperature on excess returns for brown portfolios and positive effects for green portfolios. He also derives optimal climate policy from a DSGE model. While this study in contrast to our analysis allows for model uncertainty, we allow for macroeconomic and climatic disasters. Using exogenous climate dynamics, Bansal et al. (2017, 2019) quantify the impact of local temperature on asset prices. They study a global long-run risk model that simultaneously matches the observed temperature and consumption growth dynamics. Furthermore, their model can generate a low risk-free interest rate and a high equity premium. Similar results are obtained by Donadelli et al. (2017). Karydas and Xepapadeas (2019) study an economy with two assets, but focus on a Lucas-tree endowment economy where the agent cannot actively control the transition to a low-carbon economy. By contrast, van den Bremer and van der Ploeg (2021) study a one-sector production economy with endogenous climate change and a wide range of economic and climatic uncertainties that generates low risk-adjusted interest rates and a high risk premium. Like Lemoine (2021) they find that the effect of covariance between climate shocks and economy shocks depends on whether the coefficient of relative risk aversion exceeds one or not. Dietz et al. (2018) define the "climate beta" to be the elasticity of damages with respect to economy activity and show that the optimal carbon price is increasing in this quantity. Finally, Daniel et al. (2019) show in an asset pricing setting that recursive preferences with general resolution of uncertainty about climate change can lead to a declining carbon price.[3]

Bolton and Kacperczyk (2021a) find using U.S. data that stocks of companies with higher emissions earn higher returns, even after controlling for size, book to market, momentum and other factors that predict returns. Such carbon risk premia cannot be explained by unexpected profitability or other risk premia. They statistically reject the hypothesis that investors divest from “sin” stocks and also reject

[3]The feature of a declining carbon price is derived from a binomial tree with a fixed horizon.

the market inefficiency (or carbon alpha) hypothesis, which states that markets under-price carbon risk and thus green stocks earn a premium. Bolton and Kacperczyk (2021b) confirm these results for global stock market returns. We also find such a carbon risk premium in our simulations as investors demand compensation for the tipping risk in economic damages which increases with temperature. So long as policy makers are not fully tackling climate change, there is a risk that they will tip into action and step-up climate policy. There is also a probability of a breakthrough in renewable energy or of social tipping with societies abruptly moving from carbon-intensive to carbon-free preferences. These transition risks lead to additional carbon risk premia. Donadelli et al. (2017) provide evidence that increasing awareness of the global warming challenge has led to increasing carbon risk premia. Bolton and Kacperczyk (2021b) find evidence of rising carbon risk premia for carbon-intensive stocks. The evidence suggests that markets have started to price in the climate transition from 2015 onwards. Giglio et al. (2021) reviews the interactions between climate change and financial markets for a wide variety of assets and explains how these assets can be used to hedge against climate risk.

The remainder is organized as follows. Section 2 introduces the model setup. Section 3 explains our approach to solving for the social optimum and discusses how the social optimum can be decentralized in the market economy. Section 4 discusses our calibration strategy. Section 5 presents our main results on the relation between the diversification motive and climate action. Section 6 discusses how climate change affects the equilibrium risk-free rate and the risk premia in the economy. Section 7 concludes. An online appendix provides proofs, calibration details, further simulation results, and robustness checks.

2 A Two-Sector Model of the Economy and the Climate

We present a dynamic two-sector AK-economy. The green sector uses carbon-free energy as input; the carbon-emitting sector deploys fossil fuel leading to emissions, warming and damages to aggregate output. Temperature depends on cumulative carbon emissions. Energy inputs are available at a cost. The economy can reallocate capital from the dirty to the green capital stock which is also costly. Households have recursive preferences so that risk aversion can be disentangled from the elasticity of intertemporal substitution.

2.1 Production of Goods

Final goods produced in the two sectors are perfect substitutes.[4] The capital stocks are broad measures that aggregate physical capital, human capital, and non-tangible capital such as patents. Outputs of both sectors follow from the Cobb-Douglas production functions

$$Y_n = A_n K_n^{1-\eta_n} F_n^{\eta_n} \Lambda_n(T), \qquad n \in \{1,2\},$$

where K_n is the capital stock of sector n. The rate of energy use in sector n is denoted by F_n where we refer to F_1 as *green energy* and to F_2 as *fossil fuel use*. The Cobb-Douglas weight η_n as well as total factor productivity A_n are non-negative, sector-specific constants. Here, T denotes global average temperature relative to the beginning of the industrial revolution, so $T = 0$ is the pre-industrial level of temperature. The function Λ_n is a sector-specific damage function and shows how much output is curbed in response to higher temperatures (e.g., Nordhaus and Sztorc 2013). This is the *first channel* by which global warming affects economic activity.

2.2 Investments in Green and Dirty Capital

Let $I_n \geq 0$ be the investment rate in sector n and $R \geq 0$ the rate at which carbon-emitting capital is converted into green capital.[5] Investment is subject to quadratic intertemporal adjustment costs. To convert dirty into green capital, the green sector incurs quadratic intrasectoral adjustment costs. A dollar of dirty capital is thus converted into less than a dollar of green capital and the wedge increases in the amount converted. Depreciation rates of the capital stocks are $\delta_n^k \geq 0$, $n \in \{1,2\}$. The capital stock dynamics of the green and dirty sector are thus[6]

$$\mathrm{d}K_1 = \Big(I_1 - \frac{1}{2}\phi_1 \frac{I_1^2}{K_1} + R - \frac{1}{2}\kappa \frac{R^2}{K_1} - \delta_1^k K_1\Big)\mathrm{d}t + K_1\sigma_1 \mathrm{d}W_1 - K_{1-}\Big(\ell_e \mathrm{d}N_e + \ell_c \mathrm{d}N_c\Big), \tag{2.1}$$

[4] In Appendix G.1 we relax the assumption of perfect substitutes and adopt a more involved structure with imperfect substitution between the two sectors. We then interpret Y_n as intermediate goods that are aggregated via CES into a final good $Y = \big(Y_1^\rho + Y_2^\rho\big)^{\frac{1}{\rho}}$ for a parameter $\rho \in (0,1]$, which determines the elasticity of substitution between the two sectors. We also adopt a setting where aggregate consumption is a CES-aggregate consisting of the two consumption goods produced in each sector. These extensions do not significantly affect our main results. This specification of the economic structure is rudimentary since there may be a third capital stock which is complementary to the other two capital stocks when modeling transport and the power industry separately.

[5] The constraint $R \geq 0$ implies that conversion is only feasible from the brown into the green capital stock. We choose the conversion to be one-way since we are concerned with the optimal transition to a carbon-free economy. If we allow for two-way reallocation, the optimal plan is almost never to convert from green into dirty capital (results available upon request).

[6] For notational convenience, we drop the time index t when it does not create confusion. Furthermore, K_{n-} is short for K_{nt-}, i.e., for the left-limit of K_n at time t. For the $\mathrm{d}t$ and $\mathrm{d}W$ terms this distinction is irrelevant since the point process N only jumps at countably many time points and Lebesgue and Brownian integrands can be changed at countably many points.

$$\mathrm{d}K_2 = \Big(I_2 - \frac{1}{2}\phi_2 \frac{I_2^2}{K_2} - R - \delta_2^k K_2\Big)\mathrm{d}t + K_2\sigma_2\Big(\rho_{12}\mathrm{d}W_1 + \sqrt{1-\rho_{12}^2}\mathrm{d}W_2\Big) - K_{2-}\Big(\ell_e \mathrm{d}N_e + \ell_c \mathrm{d}N_c\Big), \tag{2.2}$$

where ϕ_n, $n = 1,2$, are the investment adjustment cost parameters, κ is the capital reallocation cost parameter, and W_1 and W_2 are two independent Brownian motions. The parameter ρ_{12} denotes the instantaneous correlation coefficient between the Brownian shocks of the two capital stocks. N_e and N_c are two independent point process capturing economic and climate disaster risk. Since these disaster shocks are identical for both types of capital in realization, not just in distribution, they significantly increase the total correlation between the two capital stocks.[7]

The process N_e models macroeconomic disasters whose jump intensity λ_e is constant as in Barro (2006, 2009) and Barro and Jin (2011). The process N_c models climate disasters as in Karydas and Xepapadeas (2019). This is the *second channel* by which global warming curbs economy. Its jump intensity $\lambda_c = \lambda_c(T)$ depends on current temperature T. In both cases, $\lambda_i \mathrm{d}t$ is the probability for a jump to occur over the small time interval $\mathrm{d}t$ and $1/\lambda_i$ is the expected waiting time to the next jump, $i \in \{e,c\}$. The parameters ℓ_e and ℓ_c are the corresponding jump sizes which are stochastic, but independent of the Brownian and Poisson shocks in the model. We suppose that jump sizes are the same for both types of capital.

Climate damages thus affect the economy via the damage functions $\Lambda_n(T)$ scaling down output in response to climate change as in the DICE model and via the disaster probability increasing in temperature as in Bansal et al. (2019) and Karydas and Xepapadeas (2019). We thus assume that the size of the climate-related disasters does not increase with global warming.

2.3 Emissions and Temperature

Following Allen et al. (2009), Matthews et al. (2009), and IPCC (2014), we assume that global average temperature T increases linearly in cumulative emissions $E_t = \int_0^t \varepsilon_s \mathrm{d}s$ measured in gigatons of carbon (GtCs) and by some stochastic shocks. Global mean temperature is thus

$$T_t = T_0 + \vartheta E_t + \int_0^t \sigma_T \mathrm{d}W_{3s},$$

[7] Geometric Brownian shocks to the capital stock have been commonly used in the literature for AK-models like ours. Using Itô's lemma, it can be verified that these shocks are equivalent to having deterministic consumption dynamics and geometric Brownian shocks to total factor productivity. Following Pindyck and Wang (2013), Barro (2006, 2009), and van den Bremer and van der Ploeg (2021), among others, it is common in continuous-time models to put the geometric Brownian shocks and disaster shocks into the capital dynamics. Geometric Brownian shocks can also be interpreted as a stochastic depreciation of capital (Pindyck and Wang 2013). These shocks are the typical stochastic drivers of total factor productivity and depreciation and thus of economic growth and of asset returns. Since, in contrast to these papers, we study a two-sector model, those shocks represent correlated sectoral level shocks. Hence, total correlation between the two sectors involves instantaneous correlation from geometric Brownian shocks and common jump risk (see Section 4.1).

where T_0 is current temperature and ϑ denotes the transient climate response to cumulative emissions (TCRE). W_3 denotes a third standard Wiener process that is independent of W_1 and W_2 and has a constant diffusion coefficient σ_T. Current emissions are $\varepsilon = \nu F_2$ where F_2 is the rate of fossil use in energy units and $\nu = \nu(t, T, K_1, K_2)$ the emission intensity per unit of fossil fuel, which may depend on the current state of the world. Hence, we have

$$\mathrm{d}T = \beta F_2 \mathrm{d}t + \sigma_T \mathrm{d}W_3, \tag{2.3}$$

where $\beta = \vartheta\nu$ and thus β depends on t, T, K_1, and K_2. Note that $\varepsilon = 0$ if $K_2 = 0$, so carbon emissions cease once the dirty capital stock has been fully phased out.

2.4 Dividends, Consumption, and Preferences

The consumption good in each sector is the cash flow net of investments and energy costs,

$$C_n = Y_n - I_n - \frac{b_n (F_n/K_n)^{1/\varepsilon_n}}{1 + 1/\varepsilon_n} F_n,$$

where b_1 and b_2 are cost parameters for green energy and fossil fuel and ε_n is the price elasticity of supply in sector n. Dividends in each sector are defined as levered consumption $D_n = C_n^{\varphi}$ for a leverage parameter $\varphi > 1$ to model a higher volatility of dividends compared to consumption (e.g., Bansal and Yaron 2004; Benzoni et al. 2011; Wachter 2013; Branger et al. 2016). The representative household has recursive preferences and consumes $C = C_1 + C_2$. As shown in Duffie and Epstein (1992b), these preferences are the continuous-time version of discrete-time recursive utility developed in Kreps and Porteus (1978) and Epstein and Zin (1989). The value function J is recursively defined by

$$J(t, K_1, K_2, T) = \sup_{I_1, I_2, R, F_1, F_2} \mathbb{E}_t \Big[\int_t^{\infty} f\big(C_s, J(s, K_{1s}, K_{2s}, T_s)\big) \mathrm{d}s \Big], \tag{2.4}$$

where the aggregator function f is defined by

$$f(C, J) = \begin{cases} \delta\theta J \Big[\frac{C^{1-1/\psi}}{[(1-\gamma)J]^{1/\theta}} - 1 \Big], & \psi \neq 1, \\ \delta(1-\gamma) J \log\Big(\frac{C}{[(1-\gamma)J]^{\frac{1}{1-\gamma}}} \Big), & \psi = 1, \end{cases}$$

where $\theta = \frac{1-\gamma}{1-1/\psi}$, C denotes consumption, γ the coefficient of relative risk aversion, ψ the elasticity of intertemporal substitution (EIS), and δ the rate of time impatience. The degree of risk aversion γ typ-

ically exceeds $1/\psi$ to reflect a preference for early resolution of uncertainty. For $\gamma = 1/\psi$, the preference structure collapses to time-additive CRRA utility.

3 Optimality and the Social Cost of Carbon

Following Duffie and Epstein (1992b), the value function $J = J(t, K_1, K_2, T)$ satisfies the Hamilton-Jacobi-Bellman (HJB) equation (A.1). The first-order optimality conditions give rise to efficiency conditions (3.1) – (3.4). Optimal investment in sector $n \in \{1,2\}$ reads

$$I_n = \frac{K_n}{\phi_n} \frac{q_n - 1}{q_n}. \tag{3.1}$$

The higher ϕ_n, the higher adjustment costs and the less the sensitivity of the investment rate to the marginal value of investment. Here Tobin's Q of sector n is

$$q_n = \frac{C^{1/\psi}}{\delta} \frac{J_{K_n}}{[(1-\gamma)J]^{1-1/\theta}}. \tag{3.2}$$

Condition (3.1) shows that the investment rate in sector n is small if intertemporal adjustment costs are high and large if the sectoral Tobin's Q is high, where the latter is the marginal value of capital in utility units (i.e., J_{K_n}) divided by the marginal utility of consumption (i.e., $f_C(C,J)$) to obtain the marginal value of capital in units of consumption or final goods. The sectoral Tobin's Q, the ratio between the market value and the replacement cost of physical capital, is bigger than one, since installing capital is costly and installed capital earns a rent. The optimal reallocation from dirty to green capital is

$$R = \frac{K_1}{\kappa} \frac{q_1 - q_2}{q_1}. \tag{3.3}$$

If the marginal value of investments in the clean sector exceeds those in the dirty sector (i.e. the Tobin's Q for the green sector exceeds the one for the dirty sector), it is optimal to reallocate capital from the dirty to the green sector. The extent to which this is done increases in the gap between the Tobin's Q's and decreases in the intra-sectoral adjustment cost parameter κ, i.e., the conversion rate is small if intratemporal adjustment costs are high.

The optimal use of green energy and fossil fuel follow from

$$\eta_1 A_1 \Big(\frac{F_1}{K_1}\Big)^{\eta_1 - 1} \Lambda_1(T) = b_1 \Big(\frac{F_1}{K_1}\Big)^{1/\varepsilon_1}, \qquad \eta_2 A_2 \Big(\frac{F_2}{K_2}\Big)^{\eta_2 - 1} \Lambda_2(T) = b_2 \Big(\frac{F_2}{K_2}\Big)^{1/\varepsilon_2} + \tau_f, \tag{3.4}$$

where the optimal Pigouvian social cost for using one unit of fossil fuel is

$$\tau_f = -\frac{\beta J_T C^{1/\psi}}{\delta[(1-\gamma)J]^{1-1/\theta}}. \tag{3.5}$$

The marginal product of the green capital stock must equal the marginal cost of one unit of green energy. The marginal product of dirty capital must equal its marginal cost plus the external effects of emitting carbon. The social cost of burning one ton of carbon or SCC is

$$\tau_c = \frac{\tau_f}{\nu} = -\frac{\vartheta J_T C^{1/\psi}}{\delta[(1-\gamma)J]^{1-1/\theta}}. \tag{3.6}$$

where ν is the emission intensity per unit of fossil fuel (see Section 2.3). The optimal SCC increases in consumption as marginal damages are proportional to aggregate economic activity (cf. Nordhaus 1991; Golosov et al. 2014; Rezai and van der Ploeg 2016; Hambel et al. 2021b).

We denote the total stock of capital by $K = K_1 + K_2$, so the share of dirty to total capital $S = \frac{K_2}{K_1+K_2}$ defines the carbon-intensity of the economy. During the energy transition the share of dirty capital S decreases over time. Appendix A shows that the value function J can be reformulated in terms T and S instead of T, K_1, and K_2 (see Proposition A.1). This significantly simplifies our numerical solution approach as described in Appendix C.1.

To replicate the social optimum in the decentralized market economy, we must price carbon (either via a global carbon tax or via a global cap-and-trade system) at a price equal to the optimal SCC. The revenue of the carbon tax is refunded in lump-sum fashion to the private sector. The carbon price thus internalizes the global warming externalities.

4 Calibration

Table 1 summarizes the calibration details. Appendix D provides additional details on the calibration.

4.1 Economic Growth

In the past, the influence of climate change on asset markets was negligible and the historical impact of climate change on the economy was, if anything, modest, at least in developed countries (e.g., Dell et al. 2009, 2012). We first calibrate production by disregarding climate damages. We then calibrate the damage specification.

	Preferences	
δ	time-preference rate (annual)	0.015
γ	coefficient of relative risk aversion	4.355
ψ	elasticity of intertemporal substitution	0.618
	Economic Model	
Y_0	initial GDP (trillion US \$)	75.8
S_0	initial share of dirty capital	0.94
A_1	green total factor productivity	0.1058
A_2	brown total factor productivity	0.1030
b_1	green energy cost parameter	4.459×10^6
b_2	fossil fuel cost parameter	2.307×10^6
ε_n	price elasticity of energy supply	1.6
η_n	energy share in production	0.066
ϕ_n	investment adjustment cost parameter	39.08
φ	dividend leverage parameter	2.8
σ_n	annual capital volatility	0.02
α_e	macroeconomic jump size parameter	8
λ_e	macroeconomic disaster intensity parameter	0.088
κ	capital reallocation cost parameter	2
ρ_{12}	instantaneous correlation	0
	Climate Model	
T_0	initial temperature (°C)	1.27
σ_T	temperature diffusion coefficient	0.015
ϑ	TCRE (°C/TtC)	1.8

Table 1: Benchmark Calibration with 2020 as base year

Capital Shocks We set annual volatility of capital diffusion risk to $\sigma_1 = \sigma_2 = 0.02$ matching the observed volatility of consumption or output (e.g., Wachter 2013). We start with a benchmark value of $\rho_{12} = 0$ for the *instantaneous correlation* between the two capital stocks.[8] Section 5 discusses the influence of this correlation and presents the effects for negative and positive ρ_{12}. Apart from instantaneous correlation ρ_{12} the correlation between the two capital stocks and, in turn, between asset prices is driven by macroeconomic disasters. Since both capital stocks are exposed to macroeconomic shocks via N_e, the total correlation between the capital stocks is significantly higher than indicated by the value of ρ_{12}. In our numerical simulations total correlation is always higher than 90%.

We assume that the recovery rates, $Z_i = 1 - \ell_i$, $i \in \{e, c\}$, have power distributions over $(0,1)$ with parameters $\alpha_i > 0$, i.e., the jump size distribution is determined by the density function $\zeta_i(Z_i) = \alpha_i Z_i^{\alpha_i - 1}$, $Z_i \in (0,1)$ (Pindyck and Wang 2013). The n^{th} moment of the recovery rate is $\mathbb{E}[Z_i^n] = \frac{\alpha_i}{\alpha_i + n}$. We follow Barro and Jin (2011) and define a disaster as an event destroying more than $\overline{\ell}_e = 10\%$ of GDP or aggregate consumption. Their historical consumption data suggest an annual disaster probability of 3.8% and average consumption loss of 20% when a disaster occurs: $\mathbb{E}[\ell_e | \ell_e > \overline{\ell}_e] = 0.2$ and $\lambda_e \int_0^{1-\overline{\ell}_e} \zeta_e(Z_e) \mathrm{d}Z_e = 0.038$. These yield $\alpha_e = 8$ and $\lambda_e = 0.088$.

[8] This is also assumed by Cochrane et al. (2007) for an endowment economy.

Production and Energy Costs Empirically, dividends are more volatile than consumption (e.g., Bansal and Yaron 2004; Wachter 2013) and dividends fall more than consumption when a disaster hits the economy. Following this literature, we set the dividend leverage parameter to $\varphi = 2.8$ leading to asset return volatilities much higher than consumption growth volatility. This allows us to set a relatively low time preference rate of $\delta = 0.015$ as in Nordhaus (2017) while still matching the equity risk premium. Ignoring the effects of climate change, the optimal SCC is zero and optimal energy use implies a linear production function $Y_n = A_n^* K_n$ of the so-called "AK" variety, with productivity

$$A_n^* = A_n^{\frac{1+1/\varepsilon_n}{1-\eta_n+1/\varepsilon_n}} \left(\frac{\eta_n}{b_n}\right)^{\frac{\eta_n}{1-\eta_n+1/\varepsilon_n}}. \tag{4.1}$$

To calibrate the elasticity of intertemporal substitution, risk aversion, adjustment costs and total factor productivity, we use a special case of our model with an aggregate capital stock. Following Pindyck and Wang (2013), we choose these parameters to match a real expected growth rate of consumption of 2%, an average consumption fraction of GDP of $C/Y = 75\%$, an initial risk-free interest rate of $r_0^f = 0.8\%$ per annum, an average equity premium of 6.6% per annum, and a Tobin's Q of $q = 1.58$. We use this data to back out a relative risk aversion of $\gamma = 4.355$, an EIS of $\psi = 0.618$, adjustment cost parameters of $\phi_1 = \phi_2 = 39.08$, and total factor productivities in (4.1) of $A_1^* = A_2^* = 0.0449$.[9]

Following van den Bremer and van der Ploeg (2021), we set the energy shares to be $\eta_n = 0.066$ and use an average global cost of fossil fuel of 540 USD per ton of carbon. We use a significantly higher average global price of green energy, i.e., 810 USD for the same amount of energy,[10] which is in line with production costs in developed countries such as Germany. Using a price elasticity of energy supply of $\varepsilon_n = 1.6$ (e.g., Png 1999, p. 110), we determine cost parameters of $b_1 = 4.459 \cdot 10^6$ and $b_2 = 2.307 \cdot 10^6$ reflecting that green energy is significantly more expensive than fossil fuel.[11] Solving (4.1) for A_n yields $A_1 = 0.1058$ and $A_2 = 0.1030$.

[9] Alternatively, one could choose a higher value for the time preference rate. Then, to match the risk-free rate of $r_0^f = 0.8\%$, a higher value of the elasticity of intertemporal substitution is needed. For instance a calibration with $\delta = 0.0247$ and $\psi = 1.5$ yields almost identical results (available upon request). Since we have no information about whether the adjustment cost and total factor productivity parameters differ for the two sectors, we assume $\phi_1 = \phi_2$ and $A_1^* = A_2^*$ in our benchmark calibration. In Appendix G.2 we consider an alternative calibration where these values differ for the two sectors.

[10] We express energy in equivalent units of carbon emitted into the atmosphere.

[11] Alternative calibrations for the cost parameters and the price elasticity of supply do not significantly affect our results (available upon request).

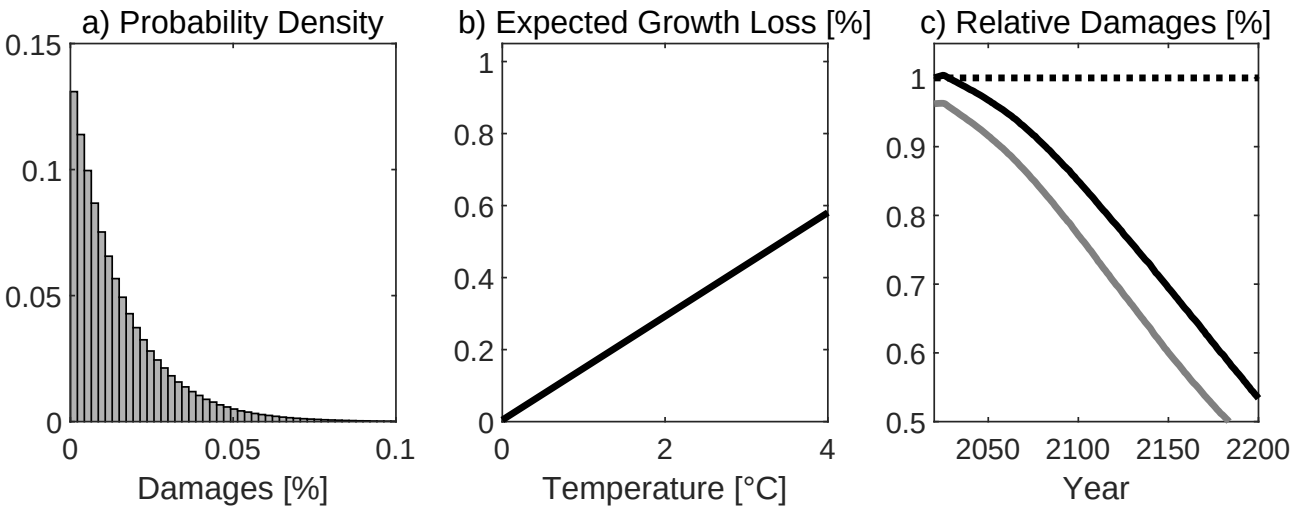

Figure 1: Disaster Impact Calibration. Panel (a) depicts the histogram of the annual damage distribution conditioned on being hit by a climate disaster from the EM-DAT database. Panel (b) relates the expected annual loss of economic growth, $\lambda_c(T)\mathbb{E}[\ell_c]$, to temperature. Panel (c) depicts the median relative damages in models with level (TFP) impact as in the DICE model and with disaster impact expressed in terms of consumption (gray line) and output (black line) in the BAU scenario. The black line depicts the median evolution of $1 - Y_t^{\text{BAU, disaster}}/Y_t^{\text{BAU, dice}}$ and the gray line depicts the median evolution of $1 - C_t^{\text{BAU, disaster}}/C_t^{\text{BAU, dice}}$.

4.2 Damage Specifications

We consider two different damage specifications.[12] For the level damage, we follow Nordhaus (2017), who uses $\Lambda_n(T) = 1 - \theta_n T^2$ and calibrates this specification such that damages at 3°C are 2.08% of pre-damages output. This gives a value of $\theta_n = 0.00236$.[13]

Karydas and Xepapadeas (2019) collect data on climate-related events for 42 countries over the period from 1911 to 2015.[14] Following the methodology of Loayza et al. (2012), they estimate climate-related disaster probabilities and magnitudes. Their model involves time-varying temperature disaster risk where the disaster intensity follows a mean-reversion process whose long-term mean is linear in temperature, $\overline{\lambda}_c(T) = \overline{\lambda}_{c0} + \overline{\lambda}_{c1} T$. Abstracting from mean reversion, we set $\lambda_c(T) = \lambda_{c0} + \lambda_{c1} T$ with $\lambda_{c0} = 0.003$ and $\lambda_{c1} = 0.096$. The process $\lambda_c(T)$ is approximately the probability that a disaster hits within the period of a year. Karydas and Xepapadeas (2019) report $\mathbb{E}[\ell_c] = 1.5\%$ for climate-related disasters. Using a power distribution for the recovery rate Z_c yields $\alpha_c = 65.67$. Figure 1 depicts the calibration of

[12] See Appendix G.3 for a model involving both types of damages.

[13] Nordhaus (2017) states that the damage function is inverse quadratic, $\Lambda_n(T) = \frac{1}{1+\theta_n T^2}$, whilst the corresponding GAMS code uses a quadratic damage function $\Lambda_n(T) = 1 - \theta_n T^2$. We have solved the model for both quadratic and inverse quadratic damage functions and the results are very similar.

[14] They use the international disasters database EM-DAT, which is available at https://www.emdat.be/

climate disasters. Panel (a) shows the distribution of climate damages if a climate disaster hits the economy. Panel (b) shows the expected annual loss of economic growth in response to higher temperatures, $\lambda_c(T)\mathbb{E}[\ell_c]$. Panel (c) shows the relative impact of climate disasters compared to the Nordhaus level damage. Due to the persistent impact on economic growth and the potentially high magnitude of damages, the disaster impact causes much more severe climate damages than the Nordhaus specification.

4.3 Climate Model

We calibrate the emission intensity ν per unit of fossil fuel such that in the business-as-usual (BAU) scenario, the model matches the RCP8.5 scenario of IPCC (2014). Historically, the emissions ratio has declined at a rate of 1.7% to 2% per year, a little less than the rate of economic growth. We model an emission intensity that steadily declines in expectation following[15]

$$\mathrm{d}\nu_t = \nu_t\Big[g_\nu \mathrm{d}t - \frac{\mathrm{d}Y_t}{Y_t}\Big],$$

where $g_\nu < \mathbb{E}\big[\frac{\mathrm{d}Y_t}{Y_t}\big]$ is a parameter determining the speed at which carbon emissions increase under BAU. Hence, carbon dioxide emissions are given by $\varepsilon_t = F_{2t}\nu_t$. This calibration ensures that carbon emissions are zero if the production of dirty goods is zero. Recent studies estimate a transient climate response to cumulative carbon emissions (TCRE) of 0.8 to 2.4°C/TtC (e.g., Allen et al. 2009; Matthews et al. 2009, 2018). We thus use a TCRE of $\beta = 1.8$°C/TtC.

Finally, we set the reallocation cost parameter to be $\kappa = 2$ so that the model predicted temperature increase in 2100 is 1.8°C for the disaster impact. This calibration is in line with the most recent pledges by the countries made at the COP26 U.N. climate conference, see IEA (2021).[16]

5 Optimal Climate Policies: To Abate or Diversify?

To understand the economic effects of our optimal carbon price paths, we discuss two opposing effects. First, dirty capital causes a negative externality that diminishes output, so the social planner seeks to cut the share of dirty capital and thus emissions. This is the *abatement motive*. Second, the social planner is risk averse, so seeks to reduce total capital volatility which is driven by the share of dirty

[15] This specification requires no extra state variable as the shocks to ν are perfectly correlated with those to Y.

[16] Since this calibration is rather indirect, κ determines the speed of the transition towards a low-carbon economy and the stickiness of investment decisions, and there is very few data on this parameter available, we perform a sensitivity analysis in Appendix G.4.

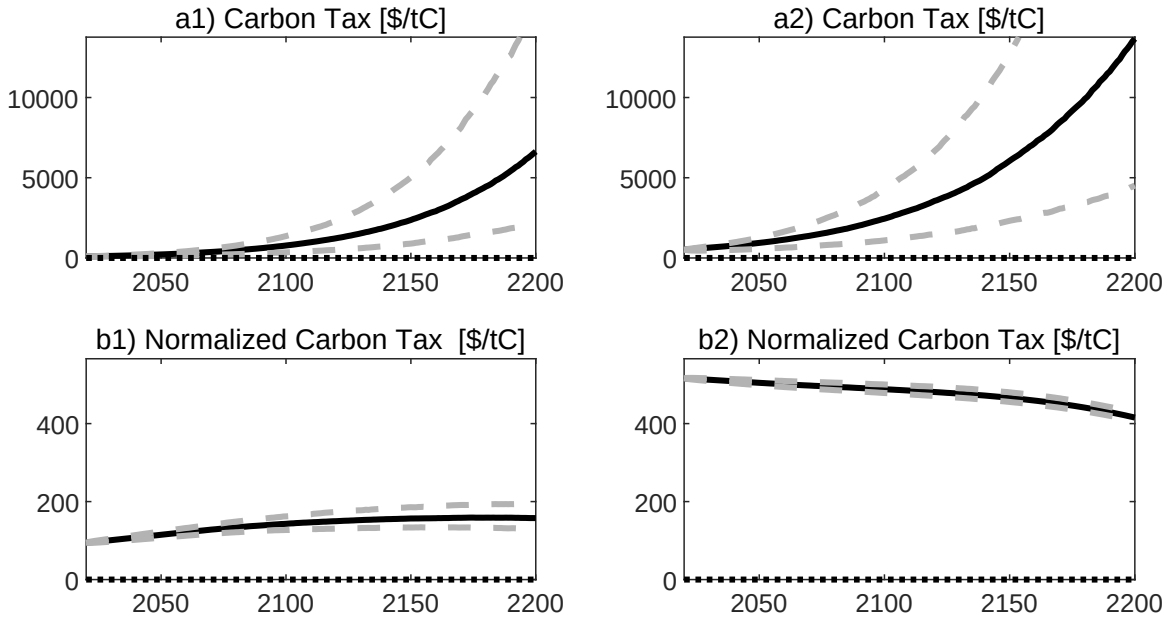

Figure 2: Optimal Carbon Taxes. The figure depicts the simulation of the optimal carbon prices for the two damage specifications level (TFP) impact (first column) and disaster impact (second column). The second row depicts carbon prices normalized for growth of the economy, i.e., $\tau_c \frac{Y_t}{Y_0}$. Median optimal paths are depicted by solid lines (——) and median BAU paths by dotted lines (·····). Dashed lines (- - -) show 5% and 95% quantiles of the optimal time paths.

capital. This is the *diversification motive*. Although we have done our best to have a calibration that fits the data and is as reasonable as the model permits, we admit that our quantitative results primarily illustrate our model and insights, and should not be taken too literally. Hence, we also offer a broad range of robustness checks in Appendix G, which discusses the drivers of the results in more detail.

A practical example of diversification might be that a solar-fueled power station has intermittent output, so one might keep open some coal-fired power stations to meet demand. A negative shock to productive capacity of the green sector might then go along with a positive shock to the carbon-intensive sector, so that the shocks are negatively correlated. There is then a diversification argument to not run the carbon-intensive sector down completely.

5.1 Optimal Carbon Prices

We first report the optimal carbon price paths. Panels a1) and a2) of Figure 2 show the median optimal carbon prices and their 5% and 95% quantiles for the benchmark cases. The optimal carbon taxes start in 2020 at 94 USD per ton of carbon (26 USD per ton of CO_2) for the level impact and at 505

USD per ton of carbon (138 USD per ton of CO_2) for the disaster impact. Since the optimal carbon tax is proportional to the aggregate stock of capital and GDP is proportional to the aggregate capital stock, the optimal carbon tax grows in line with the growth of the economy. Panels b1) and b2) of Figure 2 depict the carbon tax normalized by GDP (i.e., we multiply the carbon tax by initial GDP and divide by current GDP). This confirms that normalized carbon prices are roughly constant over time. If damages are sufficiently convex in temperature, the graph for normalized carbon prices will rise mildly as temperature increase. We now discuss the abatement and diversification motives.

5.2 Results on Abatement and Diversification

To decompose climate action into the parts that come from both motives, we consider four different model calibrations to identify a pure diversification component, a pure abatement component and an interaction term. Panel a) of Figure 3 plots the median optimal evolution of the share of dirty capital for the following calibrations: (i) a model without damages from climate change and perfectly correlated diffusive risk, see gray dotted lines (·····); (ii) a model without damages from climate change and zero instantaneous correlation, see black dotted lines (·····); (iii) a model with the Nordhaus damage specification and perfectly correlated diffusive risk, see gray lines (——); (iv) the benchmark model with the Nordhaus damage specification and zero correlation,[17] see black solid lines (——).

For calibration (i), there is neither a diversification benefit nor any damage from climate change. The planner thus has no incentive to convert brown capital into green capital. In calibration (ii), the instantaneous correlation between the two capital stocks is zero and thus diversification is advantageous. Hence, the agent aims to achieve a diversified position which due to our calibration is reached at 50% brown capital.[18] Since in this calibration there are no damages from climate change, the transition is solely driven by the diversification motive. The light gray area (■) in Panel b) depicts the diversification effect. For calibration (iii) with perfectly correlated capital stocks, there is no diversification benefit. Consequently, the transition towards a zero-carbon economy in Panel c) is solely driven by the abatement motive, which is represented by the dark gray area (■).

Finally, we study the benchmark case with zero correlation and Nordhaus damages depicted in Panel d). It turns out that the share of dirty capital optimally stabilizes in between the two polar cases (ii) and (iii). This shows that there is an interaction effect. Initially, the diversification motive fosters the

[17] The total correlation between the two capital stocks and, in turn, between asset prices is significantly driven by macroeconomic disasters. Since both capital stocks suffer common macroeconomic shocks via N^e, the total correlation between the capital stocks is significantly higher than the instantaneous diffusive correlation ρ. Our numerical simulations indicate that the total correlation is always higher than 90%.

[18] In general, if there were N energy sectors, none of which are correlated, the optimal allocation between these sectors will be $1/N$.

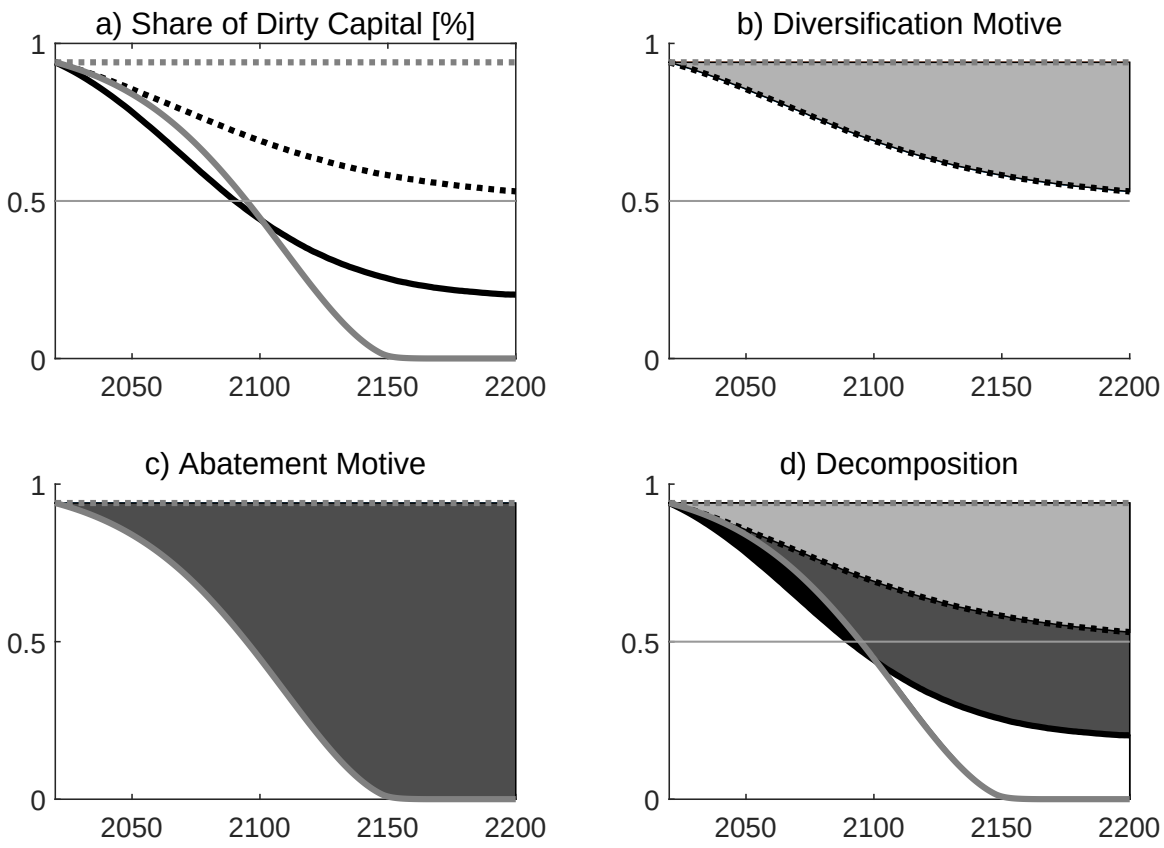

Figure 3: Abatement and Diversification Motives with Level Damages. Solid lines depict the optimal evolution of the share of dirty capital for four different calibrations until the year 2200. (i) a model without damages from climate change and perfectly correlated diffusive risk, see gray dotted lines (·····); (ii) a model without damages from climate change and zero instantaneous correlation, see black dotted lines (·····); (iii) a model with the Nordhaus damage specification and perfectly correlated diffusive risk, see gray lines (——); (iv) the benchmark model with the Nordhaus damage specification and zero correlation. The areas in b), c), and d) depict the strenghts of the diversification motive (■), the strength of the abatement motive (■), and the interaction of diversification and abatement motives (■), in scenarios (ii), (iii), and (iv), respectively.

transition towards a low-carbon economy. Compared to the case with perfect correlation, the transition takes place at a faster rate, leading to more abatement in response to diversification effects. This is visualized by the black area (■) in Panel d). In the long run, however, the two goals become conflicting and a trade-off arises. This happens around the year 2100 when the capital stocks are fully diversified. From this point onwards, the diversification motive hampers the transition, which eventually stabilizes at about 20% of dirty capital. It is thus beneficial to keep some carbon-intensive capital in the economy to reap the benefits of diversification. We thus decompose climate action into three components:

Climate Action = Diversification (■) + Abatement (■) + Interaction (■).

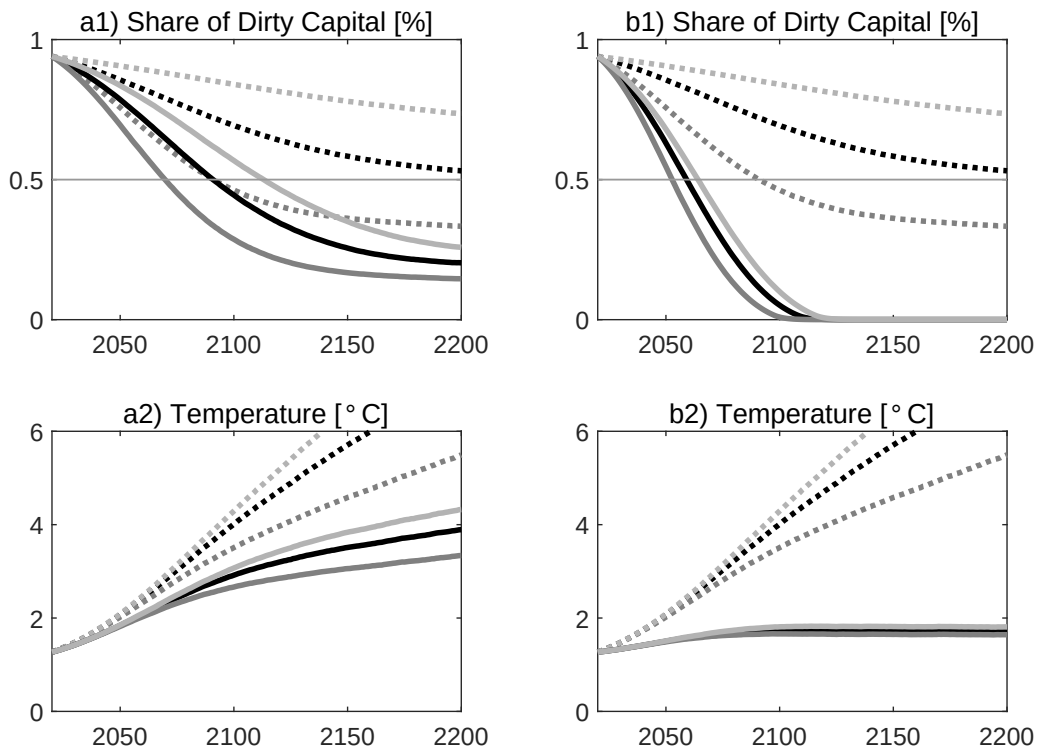

Figure 4: Heterogeneous Volatilities. Solid lines depict the optimal evolution of the share of dirty capital and global average temperature for the two damage specifications level impact (1st column) and disaster impact (2nd column) until the year 2200. Dotted lines show the results for hypothetical scenarios without damages from climate change. Black lines (⋯⋯, ——) show results for the benchmark case where the volatilities are identical. Gray lines (⋯⋯, ——) show results for a higher volatility of shocks to the dirty sector, $\sigma_2 = 0.02\sqrt{2} = 0.0282$. Light lines (⋯⋯, ——) depict the results for a lower volatility of shocks to the dirty sector, $\sigma_2 = 0.02/\sqrt{2} = 0.0141$.

This decomposition as shown in Figure 3 can be carried out for other type of damages and correlation structures too. For instance, for the disaster impact, the damages are significantly more pronounced than for the level impact, and the abatement motive dominates the diversification motive. Hence, the carbon-intensive capital stock is eventually run down completely, so that the dark gray area becomes bigger. Furthermore, a higher (lower) instantaneous correlation ρ_{12} reduces (increases) the benefit of diversification and thus lowers (increases) the level at which the share of dirty capital stabilizes in the long run (see Appendix G.6). Note that the optimal carbon prices are almost independent of the instantaneous correlation parameter ρ_{12}, which suggests that carbon prices are driven mainly by the abatement motive.

5.3 Heterogeneous Volatilities and Disaster Impact

Now, consider the effects of different capital volatilities. We fix the capital volatility of the green sector at $\sigma_1 = 0.02$ and vary the volatility of the dirty sector, $\sigma_2 \in \{0.02/\sqrt{2}, 0.02, 0.02\sqrt{2}\}$ (corresponding to "low risk", benchmark, and "high risk"). Figure 4 depicts the results. If we disregard the effects of climate change, the optimal long-term shares of the dirty sector are 2/3, 1/2, and 1/3 (dotted lines). An interesting effect arises if we take climate change into account. As can be seen from the results for the Nordhaus calibration in Panel a1), the relative reduction of the dirty sector resulting from climate damages is strongest if the volatility of the dirty sector is small, i.e., if the dirty sector has a high diversification potential ("low risk") without damages from climate change (····· vs. ——). In this case, the optimal share of the dirty sector drops from 66% to 26%. In the benchmark case, this share is 20% instead of 50%. In the high-risk scenario, the optimal share of the dirty sector drops from 33% to 15%.

The reason for the more pronounced climate action in the low-risk environment becomes clear if we look at Panel a2) depicting the temperature paths. If there is no effect of climate change on capital (·····), the temperature is highest in the low-risk scenario. Therefore, the planner reacts most if damages are internalized (——). Consequently, the total effect of the abatement motive is biggest in the low-risk scenario even though the share of dirty capital and temperature are higher than in the benchmark case (·····,——). Our findings are confirmed by Panels b1) and b2) that show the reductions for a disaster impact from climate change. The abatement motive is more pronounced for a disaster impact since the economic consequences for this damage specification are much more severe than for a level impact.

6 Equilibrium Asset Prices

Here we price the green and dirty asset. We first derive the stochastic discount factor of our economy and then provide equilibrium representations of the risk premia, dividend yields, as well as of the risk-free rate. We also determine the carbon premium, which we define as the difference between the two risk premia.

6.1 Dynamics of the Stochastic Discount Factor

The information about the current value of future (uncertain) cash flows is summarized by the stochastic discount factor (SDF) or pricing kernel. If the SDF is known, we can calculate today's price of any given cash-flow stream. It generalizes standard discount factor ideas (e.g., Cochrane 2005, pp. 6ff). Duffie and

Epstein (1992a) and Duffie and Skiadas (1994) show that for continuous-time recursive utility the SDF has the form

$$H_s = \exp\left(\int_0^s f_J(C_u, J_u)\,du\right) f_C(C_s, J_s), \tag{6.1}$$

where J_s denotes the time-s value of the value function. Applying Ito's lemma to (6.1) gives

$$\frac{\mathrm{d}H}{H_-} = \frac{\mathrm{d}f_c(C_-, J_-)}{f_c(C_-, J_-)} + f_J(C, J)\mathrm{d}t, \tag{6.2}$$

where subscripts of f denote partial derivatives and J denotes the value function whose closed-form representation is given in Proposition A.1. Although the dynamics of the SDF have the compact representation (6.2), determining the explicit form involves several auxiliary calculations (see Appendix B.1). These dynamics contain several pieces of relevant information about key variables of the economy. Its drift rate equals the equilibrium risk-free interest rate (with negative sign) and the coefficients in front of the Brownian shocks contain the market prices of diffusive risk, see Proposition 6.1 below.

Proposition 6.1 (Equilibrium)**.** *Let $\sigma_k(S_t)$ be the three-dimensional volatility vector of the total stock of capital, see (A.11), and $\sigma_g(t, S_t, T_t)$ the three-dimensional volatility vector of G, see (B.2). Let $\mu_C(t, S_t, T_t)$ and $\sigma_C(t, S_t, T_t)$ denote the drift rate and the three-dimensional volatility vector of aggregate consumption, respectively, see (B.4) and (B.5). The SDF follows the dynamics*

$$\frac{\mathrm{d}H}{H_-} = -r^f\,\mathrm{d}t + \Theta_W^\top \mathrm{d}W + \sum_{i\in\{e,c\}} \left((1-\ell_i)^{-\gamma} - 1\right)\mathrm{d}N_i - \Theta_N \mathrm{d}t$$

with $W = (W_1, W_2, W_3)^\top$. The equilibrium risk-free rate r^f is

$$\begin{aligned} r_t^f = {} & \underbrace{\delta + \frac{1}{\psi}\mu_C - \frac{1}{2}\gamma\left(1 + \frac{1}{\psi}\right)\|\sigma_C\|^2}_{\text{standard diffusion risk}} + \underbrace{\sum_{i\in\{e,c\}} \lambda_i(T)\mathbb{E}\left[(1-\ell_i)^{-\gamma} - 1 + \frac{\psi^{-1}-\gamma}{1-\gamma}\left(1-(1-\ell_i)^{1-\gamma}\right)\right]}_{\text{disaster risk}} \\ & \underbrace{+ \frac{\gamma\psi - 1}{2\psi^2}\left(\|\sigma_C - \sigma_k\|^2 + \psi\left(\|\sigma_C\|^2 - \|\sigma_k\|^2\right)\right) + \frac{\theta - 1}{\psi\theta}\sigma_g^\top(\sigma_C - \sigma_k)}_{\text{temperature interaction risk}} \end{aligned} \tag{6.3}$$

where $\|\cdot\|$ is the Euclidean norm. The market prices of diffusion risk and jump risk are

$$\Theta_{Wt} = \underbrace{-\gamma\sigma_C}_{\text{standard risk}} + \underbrace{\frac{\theta-1}{\theta}\sigma_g + \left(\gamma - \frac{1}{\psi}\right)(\sigma_C - \sigma_k)}_{\text{temperature risk}}, \qquad \Theta_{Nt} = \sum_{i\in\{e,c\}} \lambda_i(T_t)\mathbb{E}[(1-\ell_i)^{-\gamma} - 1].$$

Proposition 6.1 offers a similar decomposition of the risk-free interest rate as in Barro (2006, 2009), Pindyck and Wang (2013), and Wachter (2013). The first two terms in equation (6.3) also arise in deterministic models: if the time preference rate δ is high, there are strong preferences for early consumption and one would thus like to borrow. Since, in equilibrium, the risk-free asset is in zero net supply, the risk-free rate must increase to counter this. Besides, the risk-free rate increases in the expected growth rate of consumption μ_C due to the agent's attitude towards smooth consumption streams, which is driven by the elasticity of intertemporal substitution.

The third term $\frac{1}{2}\gamma\big(1+\frac{1}{\psi}\big)\|\sigma_C\|^2$ in equation (6.3) represents the motive for precautionary savings in response to diffusion risk, which requires the interest rate to fall to keep the risk-free asset in zero net supply. The expected consumption growth rate and its volatility depend non-linearly on both the temperature and the dirty capital share, whereby the result is more involved and qualitatively different from one-tree endowment economies.

The fourth term $\sum_{i\in\{e,c\}}\lambda_i(T)\mathbb{E}\big[(1-\ell_i)^{-\gamma}-1+\frac{\psi^{-1}-\gamma}{1-\gamma}\big(1-(1-\ell_i)^{1-\gamma}\big)\big]$ in equation (6.3) reflects precautionary savings in response to disaster risk. As for standard diffusion risk, these terms reduce the interest rate to keep the risk-free asset is in zero net supply. The greater the risk aversion, the greater is this effect, see also the extensive discussion in Wachter (2013). A novel feature is that the jump intensity for climate disaster risk λ_c increases in temperature, so that higher temperatures curb the risk-free interest rate.

The terms in the second row in equation (6.3) capture the interdependence between capital, consumption, temperature, and the value function. Compared to Cochrane et al. (2007) these terms are new and result from the inability to hedge temperature shocks. They represent precautionary savings for uninsurable temperature risk. We emphasize that these components depend on the relevant state variables, in particular on temperature, in a nonlinear manner. In case of time-additive CRRA-utility ($\gamma = 1/\psi$), these terms add up to zero. We calculate these variables numerically using finite differences, see Appendix C.2. An extensive discussion of these effects in our calibrated model is given in Section 6.3.

6.2 Pricing Dividend Claims

We use the representation of the pricing kernel to calculate the ex-dividend price P_n of both assets in the economy. For the dividend stream D_n, the time-t price of asset n equals

$$P_{nt} = \mathbb{E}_t\Big[\int_t^\infty \frac{H_s}{H_t} D_{ns}\mathrm{d}s\Big]. \tag{6.4}$$

	r_f	$\frac{1}{\psi}\mu_C$	$-\frac{1}{2}\gamma\left(1+\frac{1}{\psi}\right)\|\sigma_C\|^2$
$T = 1°\text{C}$	0.88%	4.83%	–0.12%
$T = 2°\text{C}$	0.87%	4.81%	–0.12%
$T = 3°\text{C}$	0.84%	4.78%	–0.12%
$T = 4°\text{C}$	0.81%	4.76%	–0.12%
$T = 5°\text{C}$	0.77%	4.71%	–0.12%
$S = 0.05$	0.78%	4.79%	–0.19%
$S = 0.25$	0.82%	4.79%	–0.14%
$S = 0.50$	0.84%	4.79%	–0.11%
$S = 0.75$	0.81%	4.78%	–0.14%
$S = 0.95$	0.78%	4.79%	–0.19%

Table 2: Risk-free Rate Decomposition for the Year 2100. The table shows the state-dependent terms in the decomposition of the risk-free rate (6.3) for the Nordhaus level damage specification. It provides sensitivity analysis for different values of temperature and the share of dirty capital around their median values in 2100 ($S = 0.44$, $T = 2.9°\text{C}$). The constant terms in (6.3) are the time preference rate $\delta = 0.015$, the contribution of economic disasters $\lambda_e \mathbb{E}\big[(1-\ell_e)^{-\gamma} - 1 + \frac{\psi^{-1}-\gamma}{1-\gamma}\big(1-(1-\ell_e)^{1-\gamma}\big)\big] = -0.0696$, and the contribution of climate-related disasters $\lambda_c \mathbb{E}\big[(1-\ell_c)^{-\gamma} - 1 + \frac{\psi^{-1}-\gamma}{1-\gamma}\big(1-(1-\ell_c)^{1-\gamma}\big)\big] = 0$ since $\lambda_c = 0$ for the Nordhaus specification. The temperature interaction terms corresponding to the last line in (6.3) are close to zero and do not significantly contribute to the equilibrium interest rate. A similar table for the disaster impact is available upon request.

We denote the price-dividend ratio of asset n by $\Omega_n = P_n/D_n$. Its equilibrium expected excess return corresponds to the risk premium of the asset. It is the sum of its expected ex-dividend stock return, μ_{P_n}, and dividend yield, $y_n^d = \Omega_n^{-1}$, minus the risk-free interest rate, r^f, so

$$\text{rp}_{nt} = \mu_{P_n t} + y_{nt}^d - r_t^f. \tag{6.5}$$

The price-dividend ratio $\Omega_n = P_n/D_n$ satisfies the parabolic partial differential equation (B.9), which we solve numerically (see Appendices B.3 and B.4 for technical details).

6.3 Equilibrium Risk-Free Rate and Risk Premia

Results for the Damage Calibration by Nordhaus Table 2 reports the decomposition of the risk-free rate into its state-dependent parts for the year 2100. The qualitative behavior is robust over time and similar for other years. In contrast to Karydas and Xepapadeas (2019), the drift rate of the consumption process μ_C and its volatility σ_C are endogenous since, in our setup, μ_C and $\sigma_C$depend on temperature and the share of dirty capital. Note that expected consumption growth rate μ_C decreases in temperature. The negative influence of temperature reflects the impact of climate change on output echoed in other IAMs.

The consumption volatility is also state dependent. While the effect of temperature on the precautionary-savings term $-\frac{1}{2}\gamma\left(1+\frac{1}{\psi}\right)\|\sigma_C\|^2$ is negligible, the share of dirty capital has a significant influence on the

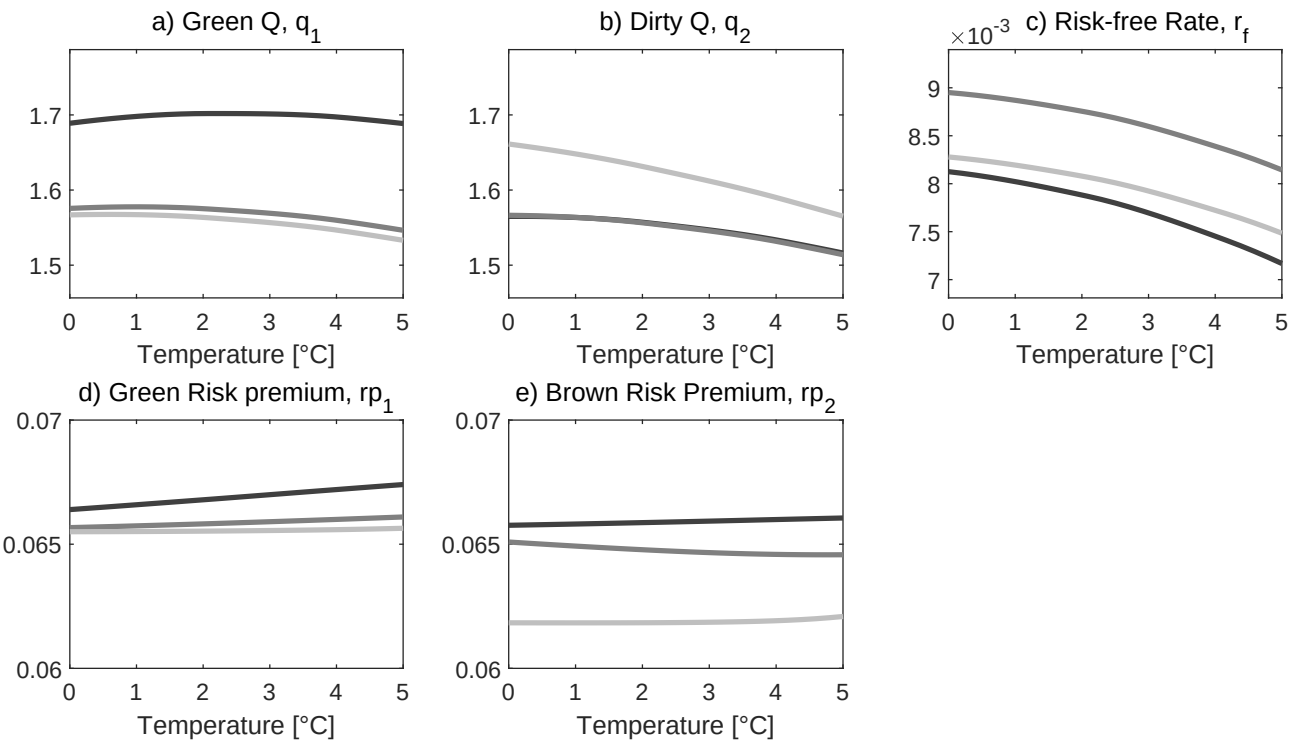

Figure 5: Asset Pricing versus Temperature and the Share of Dirty Capital (Nordhaus Damages). On the horizontal axis is temperature in the range from 0°C to 5°C. The lines represent various levels of the capital share: dark lines (——) depict $S = 0.9$, gray lines (——) refer to $S = 0.5$, and light (——) lines to $S = 0.1$. a) plots Tobin's Q of the green asset, b) shows Tobin's Q of the dirty capital stock, c) depicts the equilibrium risk-free rate, d) shows the risk premium of the green asset, e) depicts the risk premium of the dirty asset. The option to convert dirty capital into green capital generates interesting qualitative effects but the quantitative implications are moderate.

equilibrium risk-free rate. The latter result stems from a diversification argument as in Cochrane et al. (2007). Diversifying across the green and dirty capital stock reduces the volatility of the total capital stock and this effect carries over to aggregate consumption. This explains the non-monotonic behavior of the consumption volatility and, in turn, the non-monotonic relation between the share of dirty capital and the equilibrium risk-free rate.

Panels a) and b) of Figure 5 show that the Tobin's Q for both the green and the dirty sector falls with temperature. The opposite is true for the book-to-market ratio. This implies that for a fixed amount of capital the market value decreases in temperature, both for the green and dirty asset. Panel a) shows that the Tobin's Q of the green asset increases in the share of dirty capital. Therefore, for a fixed amount of capital the green asset has a higher market value if the economy is more carbon intensive. Panel b)

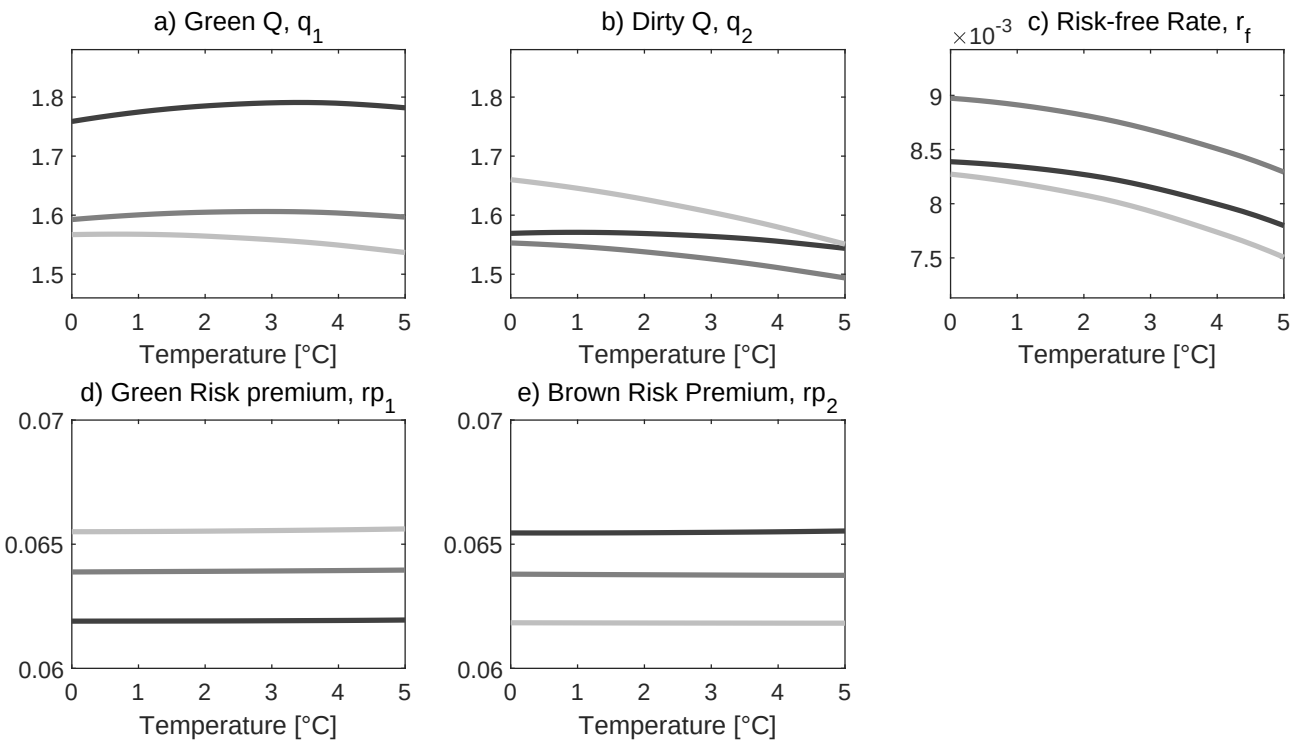

Figure 6: Asset Pricing without Option to Convert. This figure complements Figure 5 and depicts the corresponding results if the option to convert is disregarded. On the horizontal axis is temperature in the range from 0°C to 5°C. The lines represent various levels of the capital share: dark lines (——) depict $S = 0.9$, gray lines (——) refer to $S = 0.5$, and light (——) lines to $S = 0.1$. a) plots Tobin's Q of the green asset, b) shows Tobin's Q of the dirty capital stock, c) depicts the equilibrium risk-free rate, d) shows the risk premium of the green asset, e) depicts the risk premium of the dirty asset.

indicates that the opposite is true for the carbon-emitting asset. Panel c) shows the equilibrium risk-free rate, whose behavior has been discussed above.

Panels d) and e) show how the dirty and the green risk premium vary with temperature for given shares of dirty capital. Notice that the economy has the option to convert dirty into green capital at some adjustment costs. To better understand the patterns, we consider Figure 6, which is analogous to Figure 5, but disregards the option to convert. First, it can be seen in Panels d) and e) that the risk premium of the dirty and green sector is positively related to its share, S and $1-S$, respectively, which is qualitatively similar to Cochrane et al. (2007). Second, there is hardly any temperature dependence, which indicates that the variation in the shares of capital in Figure 6 is mainly driven by the diversification motive. The asset which is scarce thus carries the highest risk premium.

	Optimal				Business as usual			
	rp_1	rp_2	$y_2^d - y_1^d$	$\mathrm{rp}_2 - \mathrm{rp}_1$	rp_1	rp_2	$y_2^d - y_1^d$	$\mathrm{rp}_2 - \mathrm{rp}_1$
$T = 1°\mathrm{C}$	6.58%	6.48%	1.13%	–0.11%	6.16%	6.56%	0.55%	0.40%
$T = 2°\mathrm{C}$	6.60%	6.45%	1.58%	–0.14%	6.17%	6.57%	0.55%	0.40%
$T = 3°\mathrm{C}$	6.61%	6.44%	2.04%	–0.16%	6.17%	6.57%	0.56%	0.40%
$T = 4°\mathrm{C}$	6.62%	6.45%	2.51%	–0.17%	6.17%	6.57%	0.57%	0.40%
$T = 5°\mathrm{C}$	6.63%	6.46%	2.96%	–0.17%	6.18%	6.58%	0.57%	0.40%
$S = 0.10$	6.56%	6.20%	–0.38%	–0.35%	6.57%	6.19%	–0.36%	–0.38%
$S = 0.25$	6.61%	6.27%	0.57%	–0.34%	6.50%	6.27%	–0.19%	–0.24%
$S = 0.50$	6.61%	6.44%	2.23%	–0.17%	6.40%	6.38%	0.08%	–0.03%
$S = 0.75$	6.66%	6.53%	3.40%	–0.13%	6.29%	6.49%	0.35%	0.20%
$S = 0.90$	6.73%	6.61%	4.37%	–0.12%	6.20%	6.56%	0.53%	0.36%

Table 3: Carbon Risk Premium. The table shows the risk premia for the two assets and the carbon premium, defined as the difference between the risk premia of the two assets, for the optimal run and the business as usual scenario. It also reports the differences between dividend yields of the brown and green asset. It provides sensitivity analysis for different values of the share of dirty capital and temperature around their median values in 2100 ($S = 0.44$, $T = 2.9°\mathrm{C}$ for the optimal run and $S = 0.93$, $T = 4.4°\mathrm{C}$ for business as usual). We use the benchmark calibration from Section 4.

If the option to convert dirty capital is now taken into account, the value of the dirty asset involves the value of this option. For situations with high shares of dirty capital and currently low temperatures, the option is relatively more valuable. This can be seen in Figure 5. In turn, the green asset is relatively less valuable and the green premium is higher as long as the dirty capital share is large. Eventually, when the dirty capital share is small the brown premium is about the same with and without the option to convert, since the option has then lost its value. This becomes clear when comparing the light lines in Panel e) of Figure 5 and 6. The same is true for the green premium.

Table 3 reports the risk premia of the green and brown asset, rp_1 and rp_2, in the optimal and in the BAU scenario. It can be seen that all values are between 6.17% and 6.73%. Furthermore, the table provides the differences between these risk premia which we refer to as carbon premium, see Bolton and Kacperczyk (2021b,a). In line with this literature, we find a positive carbon premium of about 0.4% for the BAU scenario with $S = 0.9$. This carbon premium declines and becomes eventually negative if the dirty capital stock decreases. In the optimal case, society prices carbon dioxide appropriately, and thus the carbon premium is negative. Notice that variation in temperature has a minor influence on the carbon premium.

Table 3 also reports the differences between the dividend yields of the brown and green assets. From our numerical results, we know that the agent optimally invests more into the brown capital stock than in the green capital stock if the share of dirty capital is sufficiently large. Therefore, the dividends for the green asset are relatively smaller leading to a positive difference between the two dividend yields. This difference increases in the share of dirty capital and in temperature.

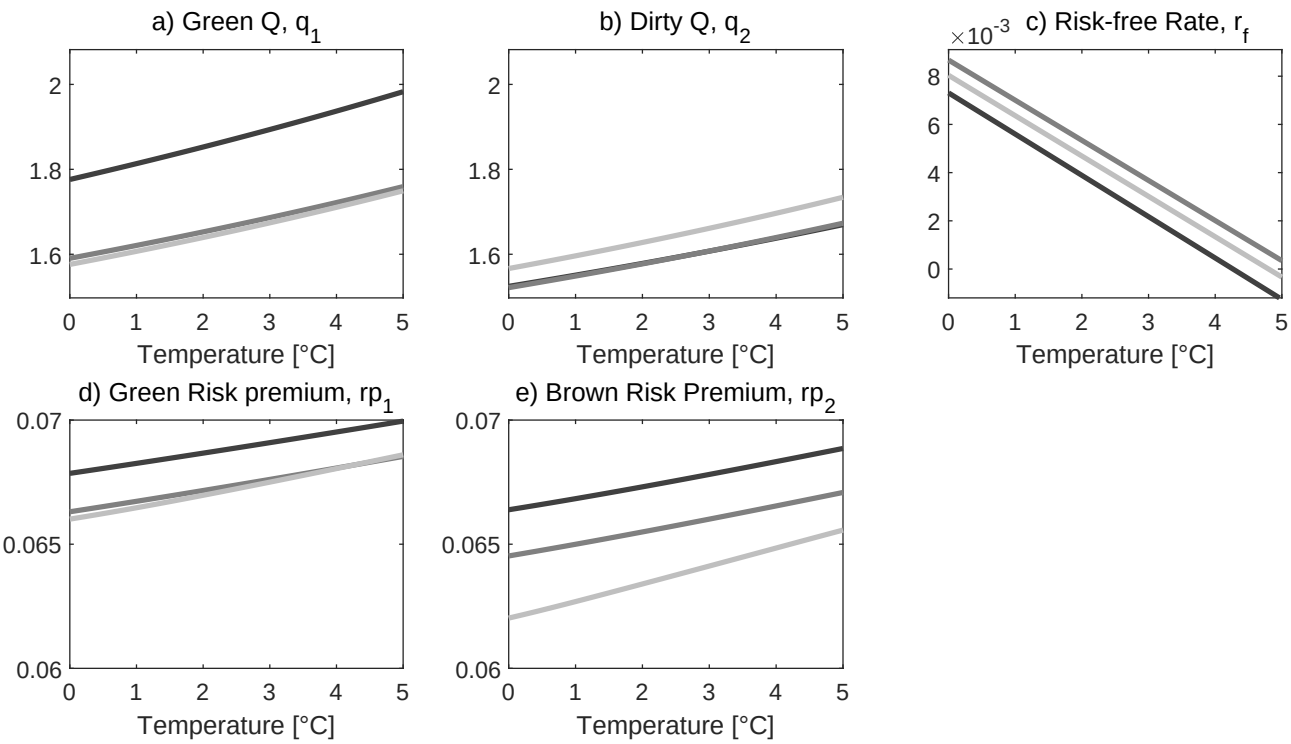

Figure 7: Asset Pricing versus Temperature and the Share of Dirty Capital (Climate Disasters). On the horizontal axis is temperature in the range from 0°C to 5°C. The lines represent various levels of the capital share: dark lines (——) depict $S = 0.9$, gray lines (——) refer to $S = 0.5$, and light (——) lines to $S = 0.1$. a) plots Tobin's Q of the green asset, b) shows Tobin's Q of the dirty capital stock, c) depicts the equilibrium risk-free rate, d) shows the risk premium of the green asset, e) depicts the risk premium of the dirty asset. The option to convert dirty capital into green capital generates interesting qualitative effects but the quantitative implications are modereate.

Results for the Damage Calibration with Climate Disasters Figure 7 depicts the asset pricing implications for the disaster impact. Since the disaster intensity grows linearly in temperature, this linearity carries over to the relevant asset pricing quantities. Most of the qualitative results obtained by the Nordhaus damage specification persist for the jump impact. The most important findings are that with climate disasters the equilibrium risk-free rate is *negatively* affected and the risk premia are positively affected by temperature. In contrast to the Nordhaus specification, economic damages involve tipping risks that increase with temperature and their magnitudes are modeled by a right-skewed power distribution. This yields another dimension of risk, for which investors want to be compensated. Furthermore, there is also a carbon risk premium in the BAU scenario as in the previous paragraph, which turns into a green premium as carbon is appropriately priced (see Table 3).

7 Conclusion

Our main concern has been the interplay between climate action and financial considerations. Since agents want to hold diversified asset holdings, the transition towards a low-carbon economy is affected by diversification motives. Diversification and climate action are initially complementary goals, since agents want to decarbonize the economy and hold a balanced portfolio of carbon-free and carbon-intensive assets. At a certain point, however, the two goals become conflicting and a trade-off arises. This is because environmental considerations incentivize the economy to further reduce the dirty capital share, but in turn assets holdings become less diversified. Climate policy is thus frustrated by the need to diversify financial asset holdings. Furthermore, if damages from climate change are moderate as in the DICE model, it is not optimal to fully run down carbon-intensive sectors as they serve as a hedge in the long run. Keeping the carbon-intensive sector open in the short run allows a faster build-up of green assets in the short run. Only if the adverse impact of global warming on economic activity is much more pronounced than suggested by DICE, it is optimal to close down the carbon-intensive sector.

We have also analyzed the dynamics of risk premia and the risk-free rate during the transition towards a low-carbon economy. We show that the existence of potential climate disasters is crucial for finding a significant effect of climate change on asset prices. Without climate disasters, the effect of climate change on asset prices is moderate. From the perspective of policy makers, our results suggest that initially policy makers should be intrinsically motivated to take climate action, simply to reach diversified asset holdings. Only if policy makers want to speed up the process, they must take extra action. Later in the transition process matters change fundamentally. If policy makers wish to incentivize the economy to reduce the carbon-intensive capital stock beyond its fully diversified share, they must counter the effects of diversification.

We also analyze a situation where the economy is stuck in a BAU scenario and does not take climate action. We show that compared to the optimal solution the equilibrium interest rates fall substantially and the carbon premium is higher and positive. This indicates that being stuck in BAU does not only hurt the real economy, but can also distort the allocation of capital in financial markets as interest rates and risk premia are biased.

Further research is needed to obtain empirical evidence on how climate policy affects the return on and prices of financial assets, both in sectors that make substantial use of fossil fuel and others that make more use of renewable energy. In particular, evidence is needed on the covariance of macroeconomic shocks, both normal macroeconomic shocks and climate-related disaster shocks, hitting the brown and green sectors to assess how important the asset diversification and hedging arguments are. We must also recognize that strategic complementarity is important in the energy transition. For example, if

more charging stations would be placed, there would be more demand for electrical vehicles, and the bigger production costs would cut the cost of electrical vehicles and increase demand for vehicles and charging stations. This can lead to path dependence with positive feedback loops and multiple equilibrium outcomes so that radical climate policies as well as carbon pricing are called for to move the economy from an high-emissions to a low-emissions equilibrium. Finally, future research needs to depart from the socially optimal outcomes for the global economy and consider policy uncertainty and the consequences for stranding of financial assets and the implications for returns and risk premia.[19]

References

Acemoglu, D., P. Aghion, L. Bursztyn, and D. Hemous, 2012, The environment and directed technical change, *American Economic Review* 102, 131–166.

Ackerman, F., E. A. Stanton, and R. Bueno, 2013, Epstein-Zin utility in DICE: Is risk aversion irrelevant to climate policy?, *Environmental and Resource Economics* 56, 73–84.

Allen, M. R., D. J. Frame, C. Huntingford, C. D. Jones, J. A. Lowe, M. Meinshausen, and N. Meinshausen, 2009, Warming caused by cumulative carbon emissions towards the trillionth tonne, *Nature* 458, 1163–1166.

Bansal, R., D. Kiku, and M. Ochoa, 2017, Price of long-run temperature shifts in capital markets, *Working Paper,* Duke University.

Bansal, R., D. Kiku, and M. Ochoa, 2019, Climate change and growth risks, *Working Paper,* Duke University.

Bansal, R., and A. Yaron, 2004, Risks for the long run: A potential resolution of asset pricing puzzles, *Journal of Finance* 59, 1481–1509.

Barnett, M., 2020, Climate change and uncertainty: An asset pricing perspective, *Working Paper,* Arizona State University.

Barnett, M., W. Brock, and L.P. Hansen, 2020, Pricing uncertainty induced by climate change, *Review of Financial Studies* 33, 1024–1066.

Barro, R. J., 2006, Rare disasters and asset markets in the twentieth century, *Quarterly Journal of Economics* 121, 823–866.

[19] A survey of stranded carbon-intensive assets is provided by van der Ploeg and Rezai (2020).

Barro, R. J., 2009, Rare disasters, asset prices, and welfare costs, *American Economic Review* 99, 243–264.

Barro, R. J., and T. Jin, 2011, On the size distribution of macroeconomic disasters, *Econometrica* 79, 1567–1589.

Benzoni, L., P. Collin-Dufresne, and R. Goldstein, 2011, Explaining asset pricing puzzles associated with the 1987 market crash, *Journal of Financial Economics* 101, 552–573.

Bolton, P., and M. Kacperczyk, 2021a, Do investors care about carbon risk?, *Journal of Financial Economics* 142, 517–549.

Bolton, P., and M. Kacperczyk, 2021b, Global pricing of carbon-transition risk, *Working Paper,* Imperial College London.

Bovenberg, A.L., and S.A. Smulders, 1996, Transitional impacts of environmental policy in an endogenous growth model, *International Economic Review* 37, 861–893.

Branger, N., H. Kraft, and C. Meinerding, 2016, The dynamics of crises and the equity premium, *Review of Financial Studies* 29, 232–270.

Bretschger, L., and A. Vinogradova, 2019, Best policy response to environmental shocks: building a stochastic framework, *Journal of Environmental Economics and Management* 97, 23–41.

Cai, Y., and T. S. Lontzek, 2019, The social cost of carbon with economic and climate risks, *Journal of Political Economy* 127, 2684–2734.

Cochrane, J. H., 2005, *Asset pricing* (Princeton University Press).

Cochrane, J. H., F. A. Longstaff, and P. Santa-Clara, 2007, Two trees, *Review of Financial Studies* 21, 347–385.

Crost, B., and C. P. Traeger, 2014, Optimal CO_2 mitigation under damage risk valuation, *Nature Climate Change* 4, 631–636.

Daniel, K., R. Litterman, and G. Wagner, 2019, Declining CO_2 price paths, *Proceedings of the National Academy of Sciences of the United States of America* 116, 20886–20891.

Dell, M., B. F. Jones, and B. A. Olken, 2009, Temperature and income: Reconciling new cross-sectional and panel estimates, *American Economic Review* 99, 198–204.

Dell, M., B. F. Jones, and B. A. Olken, 2012, Temperature shocks and economic growth: Evidence from the last half century, *American Economic Journal: Macroeconomics* 4, 66–95.

Dietz, S., C. Gollier, and L. Kessler, 2018, The climate beta, *Journal of Environmental Economics and Management* 87, 258–274.

Dietz, S., and F. Venmans, 2019, Cumulative carbon emissions andeconomic policy: In search of general principles, *Journal of Environmental Economics and Management* 96, 108–129.

Donadelli, M., M. Jueppner, M. Riedel, and C. Schlag, 2017, Temperature shocks and welfare costs, *Journal of Economic Dynamics and Control* 82, 331–355.

Duffie, D., and L. G. Epstein, 1992a, Asset pricing with stochastic differential utility, *Review of Financial Studies* 5, 411–36.

Duffie, D., and L. G. Epstein, 1992b, Stochastic differential utility, *Econometrica* 60, 353–394.

Duffie, D., and C. Skiadas, 1994, Continuous-time asset pricing: A utility gradient approach, *Journal of Mathematical Economics* 23, 107–132.

Epstein, L. G., and S. E. Zin, 1989, Substitution, risk aversion, and the temporal behavior of consumption and asset returns: A theoretical framework, *Econometrica* 57, 937–969.

Giglio, S., B. Kelly, and J. Stroebel, 2021, Climate finance, *Annual Review of Financial Economics* 13, 15–36.

Golosov, M., J. Hassler, P. Krusell, and A. Tsyvinsky, 2014, Optimal taxes on fossil fuel in general equilibrium, *Econometrica* 82, 41–88.

Hambel, C., H. Kraft, and E. S. Schwartz, 2021a, Optimal carbon abatement in a stochastic equilibrium model with climate change, *European Economic Review* 132, 103642.

Hambel, C., H. Kraft, and E. S. Schwartz, 2021b, The social cost of carbon in a non-cooperative world, *Journal of International Economics* 131, 103490.

IEA, 2021, International energy agency: World energy outlook 2021.

IPCC, 2014, *Fifth Assessment Report of the Intergovernmental Panel on Climate Change* (Cambridge University Press).

Jensen, S., and C. P. Traeger, 2014, Optimal climate change mitigation under long-term growth uncertainty: Stochastic integrated assessment and analytic findings, *European Economic Review* 69, 104–125.

Karydas, C., and A. Xepapadeas, 2019, Climate change financial risks: pricing and portfolio allocation, *Working Paper,* ETH Zurich.

Kreps, D. M., and E. L. Porteus, 1978, Temporal resolution of uncertainty and dynamic choice theory, *Econometrica* 46, 185–200.

Lemoine, D., 2021, The climate risk premium: How uncertainty affects the social cost of carbon, *Journal of the Association of Environmental and Resource Economists* 8, 27–57.

Loayza, N. V., E. Olaberra, J. Rigolini, and L Christiaensen, 2012, Natural disasters and growth: going beyond the averages, *World Development* 40, 1317–1336.

Longstaff, F. A., and M. Piazzesi, 2004, Corporate earnings and the equity premium, *Journal of Financial Economics* 74, 401–421.

Matthews, H. D., N. P. Gillett, P. A. Stott, and K. Zickfeld, 2009, The proportionality of global warming to cumulative carbon emissions, *Nature* 459, 829–832.

Matthews, H. D., K. Zickfeld, R. Knutti, and M. R. Allen, 2018, Focus on cumulative emissions, global carbon budgets and the implications for climate mitigation targets, *Environmental Research Letters* 13, 010201.

Munk, C., and C. Sørensen, 2010, Dynamic asset allocation with stochastic income and interest rates, *Journal of Financial Economics* 96, 433–462.

Nordhaus, W. D., 1991, To slow or not to slow: the economics of the greenhouse effect, *Economic Journal* 101, 920–937.

Nordhaus, W. D., 1992, An optimal transition path for controlling greenhouse gases, *Science* 258, 1315–1319.

Nordhaus, W. D., 2017, Revisiting the social cost of carbon, *Proceedings of the National Academy of Sciences* 114, 1518–1523.

Nordhaus, W. D., and P. Sztorc, 2013, DICE 2013R: Introduction and user's manual, *Technical Report,* Yale University.

Pindyck, R. S., and N. Wang, 2013, The economic and policy consequences of catastrophes, *American Economic Journal: Economic Policy* 5, 306–339.

Png, I., 1999, *Managerial Economics* (Blackwell).

Rezai, A., and F. van der Ploeg, 2016, Intergenerational inequality aversion, growth and the role of damages: Occam's rule for the global carbon tax, *Journal of the Association of Environmental and Resource Economics* 3, 499–522.

Scheffers, B., L. De Meester, T. Bridge, A. Hoffmann, J. Pandolfi, R. Corlett, S. Butchart, P. Pearce-Kelly, K Kovacs, D. Dudgeon1, M. Pacifici, C. Rondinini, W. Foden, T. Martin, C. Mora, D. Bickford, and J. Watson, 2019, The broad footprint of climate change from genes to biomes to people, *Science* 354, 719–732.

Traeger, C., 2019, Ace–analytic climate economy (with temperature and uncertainty), *Working Paper,* University of Oslo.

van den Bijgaart, I., R. Gerlagh, and M. Liski, 2016, International aspects of pollution control, *Journal of Environmental Economics and Management* 77, 75–96.

van den Bremer, T. S., and F. van der Ploeg, 2021, The risk-adjusted carbon price, *American Economic Review,* 111, 2782–2810.

van der Ploeg, F., 2018, The safe carbon budget, *Climatic Change* 147, 47–59.

van der Ploeg, F., and A. Rezai, 2019, Simple rules for climate policy and integrated assessment, *Environmental and Resource Economics* 72, 77–108.

van der Ploeg, F., and A. Rezai, 2020, Stranded assets in the transition to a carbon-free economy, *Annual Review of Resource Economics* 12:4, 1–18.

Wachter, J. A., 2013, Can time-varying risk of rare disasters explain aggregate stock market volatility?, *The Journal of Finance* 68, 987–1035.

For Online Publication: Appendix to

Asset Diversification versus Climate Action

Current version: March 23, 2022

Abstract: This online appendix contains additional material such as proofs, details of the calibration, and robustness checks.

A The Reduced-Form Value Function

A.1 Reduced-Form Value Function

Following Duffie and Epstein (1992b), the value function $J = J(t, K_1, K_2, T)$ satisfies the Hamilton-Jacobi-Bellman (HJB) equation

$$\begin{aligned}
0 = \max_{I_1, I_2, R, F_1, F_2} \Big\{ & J_t + \delta\theta J \Big[\frac{\big(\sum_{n=1,2} Y_n - I_n - \frac{b_n K_n^{-1/\varepsilon_n}}{1+1/\varepsilon_n} F_n^{1+1/\varepsilon_n}\big)^{1-1/\psi}}{[(1-\gamma)J]^{1/\theta}} - 1 \Big] + J_T \beta F_2 \\
& + \frac{1}{2} J_{TT} \sigma_T^2 + J_{K_1} \Big(I_1 - \frac{1}{2}\phi_1 \frac{I_1^2}{K_1} + R - \frac{1}{2}\kappa \frac{R^2}{K_1} - \delta_1^k K_1 \Big) + \frac{1}{2} J_{K_1 K_1} K_1^2 \sigma_1^2 \\
& + J_{K_2} \Big(I_2 - \frac{1}{2}\phi_2 \frac{I_2^2}{K_2} - R - \delta_2^k K_2 \Big) + \frac{1}{2} J_{K_2 K_2} K_2^2 \sigma_2^2 + J_{K_1 K_2} K_1 K_2 \sigma_1 \sigma_2 \rho_{12} \\
& + \lambda_e \mathbb{E}[J(K_1(1-\ell_e), K_2(1-\ell_e), T) - J] + \lambda_c(T) \mathbb{E}[J(K_1(1-\ell_c), K_2(1-\ell_c), T) - J] \Big\}
\end{aligned} \tag{A.1}$$

where subscripts of J denote partial derivatives, e.g., $J_{K_1} = \frac{\partial J}{\partial K_1}$. To solve the Hamilton-Jacobi-Bellman equation (A.1), we first transform it by expressing decision variables in relative terms and reducing the number of state variables by one. Let $i_n = I_n/K_n$, $f_n = F_n/K_n$, $r = R/K_1$, $c = C/K$ denote the relative control variables. We express the value function in terms of time, total capital $K = K_1 + K_2$, share of dirty capital $S = K_2/(K_1+K_2)$, and temperature T (instead of K_1, K_2, and T). Defining $S_1 = 1-S$, $S_2 = S$, the production functions become

$$Y_n = A_n S_n K f_n^{\eta_n} \Lambda_n(T)$$

. The amounts of consumption goods produced by each sector are

$$C_n = S_n K \big[A_n f_n^{\eta_n} \Lambda_n(T) - i_n - \frac{b_n}{1+1/\varepsilon_n} f_n^{1+1/\varepsilon_n} \big].$$

Therefore, aggregate consumption satisfies

$$c = \sum_{n=1,2} S_n \big[A_n f_n^{\eta_n} \Lambda_n(T) - i_n - \frac{b_n}{1+1/\varepsilon_n} f_n^{1+1/\varepsilon_n} \big]. \tag{A.2}$$

The dynamics of the state variables can be written as

$$\begin{aligned}
\mathrm{d}K_1 &= K_{1-} \Big[\Big(i_1 - \frac{1}{2}\phi_1 i_1^2 + r - \frac{1}{2}\kappa r^2 - \delta_1^k \Big) \mathrm{d}t + \sigma_1 \mathrm{d}W_1 - \big(\ell_e \mathrm{d}N_e + \ell_c \mathrm{d}N_c \big) \Big], \\
\mathrm{d}K_2 &= K_{2-} \Big[\Big(i_2 - \frac{1}{2}\phi_2 i_2^2 - r\frac{K_1}{K_2} - \delta_2^k \Big) \mathrm{d}t + \sigma_2 \Big(\rho_{12} \mathrm{d}W_1 + \sqrt{1-\rho_{12}^2}\, \mathrm{d}W_2 \Big) - \big(\ell_e \mathrm{d}N_e + \ell_c \mathrm{d}N_c \big) \Big],
\end{aligned}$$

$$\mathrm{d}T = \widehat{\beta} f_2 \mathrm{d}t + \sigma_T(T)\mathrm{d}W_3,$$

where $\widehat{\beta} = \beta/K_2$. To shorten the notation, we write $W = (W_1, W_2, W_3)^\top$ and denote the drift of the capital stocks and temperature by μ_{K_i} and μ_T, respectively. Ito's lemma gives the dynamics of K and S

$$\begin{aligned}
\mathrm{d}S &= S(1-S)\Big[\mu_S(i_1,i_2,r,S)\mathrm{d}t + (\sigma_2\rho_{12} - \sigma_1)\mathrm{d}W_1 + \sigma_2\sqrt{1-\rho_{12}^2}\mathrm{d}W_2\Big] \\
\mathrm{d}K &= K_-\Big[\mu_K(i_1,i_2,r,S)\mathrm{d}t + [(1-S)\sigma_1 + S\sigma_2\rho_{12}]\mathrm{d}W_1 + S\sigma_2\sqrt{1-\rho_{12}^2}\mathrm{d}W_2 - \big(\ell_e \mathrm{d}N_e + \ell_c \mathrm{d}N_c\big)\Big].
\end{aligned}$$

where the drifts are given by[20]

$$\begin{aligned}
\mu_S(i_1,i_2,r,S) &= \mu_{K_2} - \mu_{K_1} + S(\sigma_1\sigma_2\rho_{12} - \sigma_2^2) + (1-S)(\sigma_1^2 - \sigma_1\sigma_2\rho_{12}) \\
\mu_K(i_1,i_2,r,S) &= (1-S)\mu_{K_1} + S\mu_{K_2}
\end{aligned}$$

We thus solve a modified HJB equation with finite differences in terms of only two (S,T) instead of three state variables (K_1,K_2,T). The following Proposition summarizes our findings.

Proposition A.1 (Value Function and Optimal Controls)**.** *Suppose $\widehat{\beta} = \widehat{\beta}(t,S,T)$. The value function (2.4) has the form*

$$J(t,K_1,K_2,T) = \frac{1}{1-\gamma}(K_1+K_2)^{1-\gamma} G\big(t,T,S(K_1,K_2)\big). \tag{A.3}$$

where G satisfies a certain HJB equation which is given in (A.10) below. The optimal reallocation strategy from dirty to clean capital is

$$r = \frac{1}{\kappa}\Big(\frac{G_S}{G_S S + (\gamma-1)G}\Big) \tag{A.4}$$

. Optimal green energy use is

$$f_1 = \Big(\frac{b_1}{\eta_1 A_1 \Lambda_1(T)}\Big)^{\frac{1}{\eta_1 - 1 - 1/\varepsilon_1}}. \tag{A.5}$$

The optimal investment strategies and fossil fuel use follow from the nonlinear equations:

$$\delta(1-\gamma)G^{1-1/\theta}c^{-1/\psi} = \big[(1-\gamma)G - G_S S\big][1-\varphi_1 i_1], \tag{A.6}$$

$$\delta(1-\gamma)G^{1-1/\theta}c^{-1/\psi} = \big[(1-\gamma)G + G_S(1-S)\big][1-\varphi_2 i_2], \tag{A.7}$$

[20] In the following we often skip the explicit dependence of μ_S and μ_K on their variables if this does not cause any confusion.

$$\delta(1-\gamma)G^{1-1/\theta}c^{-1/\psi} = -\frac{G_T\beta}{A_2\Lambda_2\eta_2 f_2^{\eta_2-1} - b_2 f_2^{1/\varepsilon}}. \tag{A.8}$$

The optimal social cost of carbon is

$$\tau_c = \frac{\vartheta C^{1/\psi}}{\delta(\gamma-1)}\frac{G_T}{G^{1-1/\theta}}, \tag{A.9}$$

where optimal consumption is (A.2).

Proof. Let $i_n = I_n/K_n$, $f_n = F_n/K_n$, $r = R/K_1$ denote the control variables in relative terms. Substituting these relative controls into (A.1) leads to the HJB equation:

$$\begin{aligned}
0 = \sup_{i_1,i_2,f_1,f_2,r} \Big\{ & \frac{\delta}{1-1/\psi}[(1-\gamma)J]^{1-1/\theta}\Big(\sum_{n=1,2} S_n(K_1+K_2)\big[A_n f_n^{\eta_n}\Lambda_n(T) - i_n - \frac{b_n}{1+1/\varepsilon_n} f_n^{1+1/\varepsilon_n}\big]\Big)^{1-1/\psi} \\
& - \delta\theta J + J_t + J_{K_1}K_1\big(i_1 - \frac{1}{2}\phi_1 i_1^2 + r - \frac{1}{2}\kappa r^2 - \delta_1^k\big) + J_{K_2}K_2\big(i_2 - \frac{1}{2}\phi_2 i_2^2 - r\frac{K_1}{K_2} - \delta_2^k\big) \\
& + \frac{1}{2}J_{K_1K_1}K_1^2\sigma_1^2 + \frac{1}{2}J_{K_2K_2}K_2^2\sigma_2^2 + J_{K_1K_2}K_1K_2\sigma_1\sigma_2\rho_{12} + J_T\beta K_2 f_2 + J_{TT}\frac{1}{2}\sigma_T(T)^2 \\
& + \lambda_e\mathbb{E}[J(K_1(1-\ell_e),K_2(1-\ell_e),T) - J] + \lambda_c(T)\mathbb{E}[J(K_1(1-\ell_c),K_2(1-\ell_c),T) - J]\Big\}
\end{aligned}$$

We conjecture that the value function has the form

$$J(K_1,K_2,T) = \frac{1}{1-\gamma}(K_1+K_2)^{1-\gamma}G\big(T,S(K_1,K_2)\big).$$

This specification implies

$$G(T,S) > 0, \qquad G_T(T,S) > 0.$$

The partial derivatives of S are $S_{K_1} = \frac{-S}{K_1+K_2}$, $S_{K_2} = \frac{1-S}{K_1+K_2}$. The relevant partial derivatives of the value function J are

$$\begin{aligned}
J_{K_1} &= K^{-\gamma}G + \frac{1}{1-\gamma}K^{1-\gamma}G_S\frac{-S}{K}, \\
J_{K_1K_1} &= -\gamma K^{-\gamma-1}G + 2K^{-\gamma}G_S\frac{-S}{K} + \frac{1}{1-\gamma}K^{1-\gamma}\Big[G_{SS}\frac{S^2}{K^2} + 2G_S\frac{S}{K^2}\Big], \\
J_{K_2} &= K^{-\gamma}G + \frac{1}{1-\gamma}K^{1-\gamma}G_S\frac{1-S}{K}, \\
J_{K_2K_2} &= -\gamma K^{-\gamma-1}G + 2K^{-\gamma}G_S\frac{1-S}{K} + \frac{1}{1-\gamma}K^{1-\gamma}\Big[G_{SS}\frac{(1-S)^2}{K^2} - 2G_S\frac{1-S}{K^2}\Big],
\end{aligned}$$

$$J_{K_1K_2} = -\gamma K^{-1-\gamma} G + K^{-\gamma} G_S \frac{1-2S}{K} + \frac{1}{1-\gamma} K^{1-\gamma} \Big[G_{SS} \frac{-(1-S)S}{K^2} + G_S \frac{2S-1}{K^2} \Big],$$

$$J_T = \frac{1}{1-\gamma} K^{1-\gamma} G_T.$$

Substituting the conjecture and its partial derivatives into the HJB equation leads to the following reduced-form HJB equation

$$0 = \sup_{i_1, i_2, f_1, f_2, r} \Big\{ G_t + M_0 + M_1 G + M_2 G_S + M_3 G_{SS} + M_4 G_T + M_5 G_{TT} \Big\} \tag{A.10}$$

We introduce the three-dimensional volatility vectors

$$\sigma_k(S) = \big((1-S)\sigma_1 + S\sigma_2\rho_{12}, S\sigma_2\sqrt{1-\rho_{12}^2}, 0 \big)^\top, \tag{A.11}$$

$$\sigma_s = \big(\sigma_2\rho_{12} - \sigma_1, \sigma_2\sqrt{1-\rho_{12}^2}, 0 \big)^\top. \tag{A.12}$$

The coefficients M_ℓ ($\ell = 1, \ldots, 5$) are given by

$$\begin{aligned}
M_0 &= \delta\theta G^{1-1/\theta} c^{1-1/\psi} \\
M_1 &= (1-\gamma)\Big[\underbrace{(1-S)\mu_1 + S\mu_2}_{=\mu_k} - \frac{1}{2}\gamma [\underbrace{(1-S)^2\sigma_1^2 + S^2\sigma_2^2 + 2S(1-S)\sigma_1\sigma_2\rho_{12}}_{=\|\sigma_k\|^2}] \Big] - \delta\theta \\
&\quad + \lambda_e \mathbb{E}[(1-\ell_e)^{1-\gamma} - 1] + \lambda_c(T)\mathbb{E}[(1-\ell_c)^{1-\gamma} - 1] \\
M_2 &= S(1-S)\Big(\mu_2 - \mu_1 - \gamma \big[\underbrace{S\sigma_2^2 - (1-S)\sigma_1^2 + (1-2S)\sigma_1\sigma_2\rho_{12}}_{=\sigma_k^\top \sigma_s} \big] \Big) \\
M_3 &= \frac{1}{2}(1-S)^2 S^2 \big[\underbrace{\sigma_1^2 + \sigma_2^2 - 2\sigma_1\sigma_2\rho_{12}}_{=\|\sigma_s\|^2} \big] \\
M_4 &= \widehat{\beta} f_2 \\
M_5 &= \frac{1}{2}\sigma_T(T)^2
\end{aligned}$$

where c is given in (A.2) and $\widehat{\beta} = \beta/K_2$. The separation thus holds if and only if $\widehat{\beta}$ is independent of K_1 and K_2, i.e., $\widehat{\beta} = \widehat{\beta}(t, T, S)$. Calculating the first-order optimality conditions leads to the nonlinear system of equations (A.4)-(A.8) that determines the optimal controls. This proves the proposition. □

B Stochastic Discount Factor and Asset Prices

B.1 Proof of Proposition 6.1

Duffie and Epstein (1992a) and Duffie and Skiadas (1994) show that the dynamics of the pricing kernel H are given by (6.2) where the relevant partial derivatives of the aggregator can be written in terms of G

$$f_c(C,J) = \delta G^{1-1/\theta} K^{-\gamma} c^{-1/\psi} \qquad f_J(C,J) = \delta(\theta-1)c^{1-1/\psi} G^{-1/\theta} - \delta\theta.$$

To calculate the dynamics of the SDF, we first compute

$$\frac{\mathrm{d}K^{-\gamma}}{K^{-\gamma}} = \Big(-\gamma\mu_k + \frac{1}{2}\gamma(\gamma+1)\|\sigma_k\|^2\Big)\mathrm{d}t - \gamma\sigma_k^\top \mathrm{d}W + \sum_{i\in\{e,c\}} \big((1-\ell_i)^{-\gamma} - 1\big)\mathrm{d}N_i.$$

Next, we determine the dynamics of $G^{1-1/\theta}$. According to Itô's lemma, G satisfies

$$\mathrm{d}G = G[\mu_g \mathrm{d}t + \sigma_g^\top \mathrm{d}W]$$

with

$$\mu_g = \frac{1}{G}\Big(G_t + G_S S(1-S)\mu_s + G_T \beta f_2 + \frac{1}{2}G_{SS}S^2(1-S)^2\|\sigma_s\|^2 + \frac{1}{2}G_{TT}\sigma_T(T)^2\Big), \tag{B.1}$$

$$\sigma_g = \frac{1}{G}\Big(G_S S(1-S)(-\sigma_1 + \sigma_2\rho_{12}),\, G_S S(1-S)\sigma_2\sqrt{1-\rho_{12}^2},\, G_T\sigma_T(T)\Big)^\top. \tag{B.2}$$

Another application of Itô's lemma yields

$$\frac{\mathrm{d}G^{1-1/\theta}}{G_-^{1-1/\theta}} = \Big[\frac{\theta-1}{\theta}\mu_g - \frac{\theta-1}{2\theta^2}\|\sigma_g\|^2\Big]\mathrm{d}t + \frac{\theta-1}{\theta}\sigma_g^\top \mathrm{d}W$$

Therefore, by Itô's product rule,

$$\begin{aligned}\frac{\mathrm{d}(G^{1-1/\theta}K^{-\gamma})}{(G^{1-1/\theta}K^{-\gamma})_-} &= \Big(-\gamma\mu_k + \frac{1}{2}\gamma(\gamma+1)\|\sigma_k\|^2\Big)\mathrm{d}t + \frac{\theta-1}{\theta}\Big(\mu_g - \gamma\langle\sigma_k,\sigma_g\rangle\Big)\mathrm{d}t \\ &\quad - \frac{\theta-1}{2\theta^2}\|\sigma_g\|^2\mathrm{d}t + \Big(\frac{\theta-1}{\theta}\sigma_g - \gamma\sigma_k\Big)^\top \mathrm{d}W + \sum_{i\in\{e,c\}}\big((1-\ell_i)^{-\gamma}-1\big)\mathrm{d}N_i.\end{aligned} \tag{B.3}$$

Notice that according to to the simplified HJB equation (A.10),

$$\mu_g - \gamma\langle\sigma_k,\sigma_s\rangle\frac{G_S}{G}S(1-S) = (\gamma-1)\big(\mu_k - \frac{1}{2}\gamma\|\sigma_k\|^2\big) + \delta\theta - \delta\theta G^{-1/\theta}c^{1-1/\psi} - \sum_{i\in\{e,c\}}\lambda_i\mathbb{E}[(1-\ell_i)^{1-\gamma}-1].$$

Substituting this term into (B.3) yields

$$\begin{aligned}\frac{\mathrm{d}(G^{1-1/\theta}K^{-\gamma})}{(G^{1-1/\theta}K^{-\gamma})_-} &= \Big(-\gamma\mu_k + \frac{1}{2}\gamma(\gamma+1)\|\sigma_k\|^2\Big)\mathrm{d}t - \frac{\theta-1}{2\theta^2}\|\sigma_g\|^2\mathrm{d}t\\ &+ \frac{\theta-1}{\theta}\Big((\gamma-1)\big(\mu_k - \frac{1}{2}\gamma\|\sigma_k\|^2\big) + \delta\theta - \delta\theta G^{-1/\theta}c^{1-1/\psi}\Big)\mathrm{d}t + \Big(\frac{\theta-1}{\theta}\sigma_g - \gamma\sigma_k\Big)^\top\mathrm{d}W\\ &+ \sum_{i\in\{e,c\}}\big((1-\ell_i)^{-\gamma}-1\big)\mathrm{d}N^i - \frac{\theta-1}{\theta}\sum_{i\in\{e,c\}}\lambda_i\mathbb{E}[(1-\ell_i)^{1-\gamma}-1]\mathrm{d}t\end{aligned}$$

The consumption-capital ratio $c = C/K$ has the following dynamics

$$\frac{\mathrm{d}c}{c} = \mu_c\mathrm{d}t + \sigma_c^\top\mathrm{d}W$$

for auxiliary functions $\mu_c(t,S,T)$ and $\sigma_c(t,S,T)$, which can be determined numerically, see Appendix C.2. In turn,

$$\frac{\mathrm{d}c^{-1/\psi}}{c^{-1/\psi}} = -\frac{1}{\psi}(\mu_c\mathrm{d}t + \sigma_c^\top\mathrm{d}W) + \frac{1+\psi}{2\psi^2}\|\sigma_c\|^2\mathrm{d}t.$$

Set $\widetilde{H} = G^{1-1/\theta}K^{-\gamma}$. Then $\mathrm{d}f_c(C,J) = \delta(\widetilde{H}_-\mathrm{d}c^{-1/\psi} + c_-^{-1/\psi}\mathrm{d}\widetilde{H} + \mathrm{d}\langle c^{-1/\psi},\widetilde{H}\rangle)$. Consequently, the pricing kernel dynamics are given by

$$\begin{aligned}\frac{\mathrm{d}H_-}{H_-} &= \frac{\mathrm{d}f_c}{f_c} + f_J\mathrm{d}t\\ &= -\Big(\delta + \frac{1}{\psi}\mu_k - \frac{1}{2}\gamma\Big(1+\frac{1}{\psi}\Big)\|\sigma_k\|^2\Big)\mathrm{d}t - \frac{1}{\psi}\mu_c + \frac{1+\psi}{2\psi^2}\|\sigma_c\|^2 + \frac{\gamma}{\psi}\sigma_c^\top\sigma_k\mathrm{d}t\\ &- \Big(\frac{\theta-1}{2\theta^2}\|\sigma_g\|^2 + \frac{\theta-1}{\psi\theta}\sigma_c^\top\sigma_g\Big)\mathrm{d}t + \Big(-\gamma\sigma_k + \frac{\theta-1}{\theta}\sigma_g - \frac{1}{\psi}\sigma_c\Big)^\top\mathrm{d}W\\ &+ \sum_{i\in\{e,c\}}\lambda_i\mathbb{E}\Big[(1-\ell_i)^{-\gamma} - 1 + \frac{\psi^{-1}-\gamma}{1-\gamma}\big(1-(1-\ell_i)^{1-\gamma}\big)\Big]\mathrm{d}t\\ &+ \sum_{i\in\{e,c\}}\Big[\big((1-\ell_i)^{-\gamma}-1\big)\mathrm{d}N^i - \lambda_i\mathbb{E}[(1-\ell_i)^{-\gamma}-1]\mathrm{d}t\Big]\end{aligned}$$

Another application of Itô's product rule yields the drift and volatility vector of optimal consumption

$$\mu_C(t,S,T) = \mu_k(S) + \mu_c(t,S,T) + \sigma_c(t,S,T)^\top\sigma_k(S), \tag{B.4}$$

$$\sigma_C(t,S,T) = \sigma_k(S) + \sigma_c(t,S,T). \tag{B.5}$$

Substituting (B.4) and (B.5) into the pricing kernel dynamics and some algebra finishes the proof. □

B.2 Dividend Dynamics

The amount of consumption goods produced in sector n are

$$C_n = Y_n - I_n - b_n F_n = c_n K_n$$

with $c_n = A_n f_n^{\eta_n} \Lambda_n(T) - i_n - \frac{b_n}{1+1/\varepsilon_n} f_n^{1+1/\varepsilon_n}$. An application of Ito's lemma shows that c_n evolves according to

$$\frac{\mathrm{d}c_n}{c_{n-}} = \mu_{c_n}\mathrm{d}t + \sigma_{c_n}^\top \mathrm{d}W$$

for auxiliary functions μ_{c_n}, σ_{c_n} that can be determined numerically along the lines of Appendix C.2. Notice that c_n is unaffected when the economy is hit by a disaster shock N^d.

Empirically, dividends are more volatile than consumption (e.g., Bansal and Yaron 2004) and dividends fall more than consumption when a disaster hits the economy (e.g., Longstaff and Piazzesi 2004). Following Wachter (2013), among others, we thus model dividends as levered consumption, i.e., $D_n = C_n^\varphi$ for $\varphi \geq 1$.[21] An application of Ito's product rule yields dividend dynamics

$$\frac{\mathrm{d}D_n}{D_{n-}} = \mu_{D_n}\mathrm{d}t + \sigma_{D_n}^\top \mathrm{d}W + \sum_{i\in\{e,c\}} [(1-\ell_i)^\varphi - 1]\mathrm{d}N^i \tag{B.6}$$

with

$$\mu_{D_n} = \varphi(\mu_{K_n} + \mu_{c_n} + \sigma_{c_n}^\top \sigma_{K_n}) + \frac{1}{2}\varphi(\varphi-1)\|\sigma_{k_n} + \sigma_{c_n}\|^2,$$
$$\sigma_{D_n} = \varphi(\sigma_{k_n} + \sigma_{c_n}).$$

[21] A popular alternative to this approach is modelling the consumption-dividend ratio as a stationary but persistent process, as in Longstaff and Piazzesi (2004), among others. In order to focus on the novel implications of climate risk on asset prices, we keep the setting simple although following this approach would also be feasible in our setting.

In a second step, we determine the dynamics of discounted dividends, $\widehat{D}_n = HD_n$. Another application of Itô's product rule implies

$$\frac{\mathrm{d}\widehat{D}_n}{\widehat{D}_{n-}} = \mu_{\widehat{D}_n}(S,T)\mathrm{d}t + \sigma_{\widehat{D}_n}(T,S)^\top \mathrm{d}W + \sum_{i\in\{c,e\}} \big((1-\ell_i)^{\varphi-\gamma}-1\big)\mathrm{d}N_i$$

with

$$\mu_{\widehat{D}_n} = \mu_H + \mu_{D_n} + \Theta_H^\top \sigma_{D_n} \qquad \text{and} \qquad \sigma_{\widehat{D}_n} = \Theta_H + \sigma_{D_n}.$$

B.3 Price-dividend Ratios of Dividend Claims

Let $\omega_n = \log\big(\frac{P_n}{D_n}\big)$ denote the log price-dividend ratio of asset n. Due to the representation (B.6) of the dividends, the dynamics of K_n (2.1, 2.2), and the pricing equation (6.4), the price is linear in D_n and thus the price-dividend ratio is independent of K_n. Therefore, it is a continuous process with dynamics

$$\frac{\mathrm{d}\omega_n}{\omega_{n-}} = \mu_{\omega_n}\mathrm{d}t + \sigma_{\omega_n}^\top \mathrm{d}W$$

where the drift and the volatility vector are given by

$$\begin{aligned}
\mu_{\omega_n} &= \frac{1}{\omega_n}\big[\omega_{n,t} + \omega_{n,S}S(1-S)\mu_S + \omega_{n,T}\mu_T + \frac{1}{2}\omega_{n,TT}\|\sigma_T\|^2 + \frac{1}{2}\omega_{n,SS}S^2(1-S)^2\|\sigma_S\|^2\big] \\
\sigma_{\omega_n} &= \frac{1}{\omega_n}\big[\omega_{n,T}\sigma_T + \omega_{n,S}S(1-S)\sigma_S\big].
\end{aligned}$$

In particular, the price-dividend ratio $\Omega_n = \mathrm{e}^{\omega_n}$ satisfies the following dynamics

$$\frac{\mathrm{d}\Omega_n}{\Omega_{n-}} = \big(\omega_n\mu_{\omega_n} + \frac{1}{2}\omega_n^2\|\sigma_{\omega_n}\|^2\big)\mathrm{d}t + \omega_n\sigma_{\omega_n}^\top \mathrm{d}W$$

We rewrite the discounted asset price HP_n as $F_n(\widehat{D}_n,\omega_n) = \widehat{D}_n\mathrm{e}^{\omega_n}$. It follows from Itô's lemma that

$$\frac{\mathrm{d}F_n}{F_{n-}} = \big(\mu_{\widehat{D}_n} + \omega_n\mu_{\omega_n} + \frac{1}{2}\omega_n^2\|\sigma_{\omega_n}\|^2 + \omega_n\sigma_{\omega_n}^\top\sigma_{\widehat{D}_n}\big)\mathrm{d}t + (\omega_n\sigma_{\omega_n} + \sigma_{\widehat{D}_n})^\top\mathrm{d}W + \sum_{i\in\{e,c\}}\big((1-\ell_i)^{\phi-\gamma}-1\big)\mathrm{d}N^i.$$

An application of the Feynman-Kač Theorem yields

$$\mathscr{L}F_n + \mathrm{e}^{-\omega_n}F_n = 0, \tag{B.7}$$

where $\mathscr{L}F_n$ denotes the infinitesimal generator. The no-arbitrage condition implies

$$\frac{\mathscr{L}F_n}{F_{n-}} = \mu_{\widehat{D}_n} + \omega_n\mu_{\omega_n} + \frac{1}{2}\omega_n^2\|\sigma_{\omega_n}\|^2 + \omega_n\sigma_{\omega_n}^\top\sigma_{\widehat{D}_n} + \sum_{i\in\{e,c\}}\lambda_i\mathbb{E}\big[(1-\ell_i)^{\phi-\gamma}-1\big]. \tag{B.8}$$

Substituting (B.8) into (B.7) yields

$$0 = \mu_{\widehat{D}_n} + \omega_n\mu_{\omega_n} + \frac{1}{2}\omega_n^2\|\sigma_{\omega_n}\|^2 + \omega_n\sigma_{\omega_n}^\top\sigma_{\widehat{D}_n} + \lambda_d\textstyle\sum_{i\in\{e,c\}}\lambda_i\mathbb{E}\big[(1-\ell_i)^{\phi-\gamma}-1\big] + \mathrm{e}^{-\omega_n}$$

Consequently, we obtain the following partial differential equation for the log price-dividend ratio ω_n:

$$\begin{aligned}0 = {}& \sum_{i\in\{e,c\}}\lambda_i\mathbb{E}\big[(1-\ell_i)^{\phi-\gamma}-1\big] + \mathrm{e}^{-\omega_n} + \mu_{\widehat{D}_n} + \omega_{n,t} + \omega_{n,S}S(1-S)\mu_S + \omega_{n,T}\mu_T + \frac{1}{2}(\omega_{n,TT}+\omega_{n,T}^2)\|\sigma_T\|^2 \\ & + \frac{1}{2}(\omega_{n,SS}+\omega_{n,S}^2)S^2(1-S)^2\|\sigma_S\|^2 + \big(\omega_{n,T}\sigma_T + \omega_{n,S}S(1-S)\sigma_S\big)^\top\sigma_{\widehat{D}_n}\end{aligned}$$

Notice that this PDE is nonlinear since it involves squared partial derivatives of ω_n. To simplify the numerical solution approach, we transform this PDE into a linear, parabolic PDE that can be solved using finite differences. We substitute $\Omega_n = \mathrm{e}^{\omega_n}$ and end up with

$$\begin{aligned}0 = {}& 1 + \Omega_n\Big(\mu_{\widehat{D}_n} + \lambda_d\mathbb{E}\big[(1-\ell)^{1-\gamma}-1\big]\Big) + \Omega_{n,t} + \Omega_{n,S}S(1-S)\mu_S + \Omega_{n,T}\mu_T + \frac{1}{2}\Omega_{n,TT}\|\sigma_T\|^2 \\ & + \frac{1}{2}\Omega_{n,SS}S^2(1-S)^2\|\sigma_S\|^2 + (\Omega_{n,T}\sigma_T + \Omega_{n,S}S(1-S)\sigma_S)^\top\sigma_{\widehat{D}_n}\end{aligned} \tag{B.9}$$

B.4 Risk Premia

The dynamics of the asset price $P_n = \mathrm{e}^{\omega_n}D_n$ follow via Itô's lemma. We obtain the following asset price dynamics

$$\frac{\mathrm{d}P_n}{P_{n-}} = \mu_{P_n}\mathrm{d}t + \sigma_{P_n}^\top\mathrm{d}W + \sum_{i\in\{c,e\}}[(1-\ell_i)^\varphi - 1]\mathrm{d}N_i - \sum_{i\in\{c,e\}}\lambda_i\mathbb{E}[(1-\ell_i)^\varphi-1]\mathrm{d}t$$

where the expected stock return and the volatility vector are given by where the expected stock return and the volatility vector are given by

$$\begin{aligned}\mu_{P_n} &= \mu_{\omega_n} + \mu_{D_n} + \sigma_{D_n}^\top\sigma_{\omega_n} + \frac{1}{2}\|\sigma_{\omega_n}\|^2 + \sum_{i\in\{c,e\}}\lambda_i\mathbb{E}[(1-\ell_i)^\varphi - 1] \\ \sigma_{P_n} &= \sigma_{\omega_n} + \sigma_{D_n}\end{aligned}$$

Now, the risk premium of asset n can be computed as the sum of its expected stock return, μ_{P_n}, and its dividend yield, $\mathrm{e}^{-\omega_n}$, minus the risk-free interest rate, r^f, i.e.,

$$\mathrm{rp}_n = \mu_{P_n} + \mathrm{e}^{-\omega_n} - r^f.$$

C Numerical Solution Approach

C.1 Value Function and Optimal Controls

Basic idea We face a problem with an infinite time horizon. Since the boundary conditions on G are unknown, we transform the problem into a similar one with a finite time horizon denoted by $t_{\max}$. In our implementation, we consider a model with a finite time horizon and set $G(t_{\max}, T, S) = 1$, which can be interpreted as that the economy consumes the whole capital stock at $t_{\max}$. Starting with this terminal condition, we work backwards through the time grid until the differences between the value function in $t+1$ and t become negligibly small and the solution converges to that of an infinite time horizon.

Definition of the grid We use a grid-based solution approach to solve the non-linear PDE. We discretize the (t, T, S)-space using an equally-spaced lattice. Its grid points are defined by

$$\big\{(t_n, T_i, S_j) \mid n = 0, \cdots, N_t,\, i = 0, \cdots, N_T,\, j = 0, \cdots, N_S\big\},$$

where $t_n = n\Delta_t$, $T_i = i\Delta_T$, and $S_j = j\Delta_S$ for some fixed grid size parameters Δ_t, Δ_T, and Δ_S that denote the distances between two grid points. The numerical results are based on a choice of $N_T = 50$, $N_S = 600$ and 1 time step per year. Our results hardly change if we use a finer grid or more time steps per year. In the sequel, $G_{n,i,j}$ denotes the approximated value function at the grid point (t_n, T_i, S_j) and $\pi_{n,i,j}$ refers to the corresponding set of optimal controls. We apply an implicit finite-difference scheme.

Finite differences approach In this paragraph, we describe the numerical solution approach in more detail. We adapt the numerical solution approach used by Munk and Sørensen (2010). The numerical procedure works as follows. At any point in time, we make a conjecture for the optimal strategy $\pi^*_{n,i,j}$. A good guess is the value at the previous grid point since the abatement strategy varies only slightly over a small time interval, i.e., we set $\pi_{n-1,i,j} = \pi^*_{n,i,j}$. Substituting this guess into the HJB equation yields a semi-linear PDE:

$$0 = \delta\theta G^{1-1/\theta} c^{1-1/\psi} + M_1 G + M_2 G_T + M_3 G_{TT} + M_4 G_S + M_5 G_{SS}$$

with state-dependent coefficients $M_i = M_i(t,T,S)$ as stated in Appendix A. Due to the implicit approach, we approximate the time derivative by forward finite differences. In the approximation, we use the so-called 'up-wind' scheme that stabilizes the finite differences approach. Therefore, the relevant finite differences at the grid point (n,i,j) are given by

$$\begin{aligned}
&\mathrm{D}_T^+ G_{n,i,j} = \frac{G_{n,i+1,j} - G_{n,i,j}}{\Delta_T}, \qquad \mathrm{D}_T^- G_{n,i,j} = \frac{G_{n,i,j} - G_{n,i-1,j}}{\Delta_T},\\
&\mathrm{D}_S^+ G_{n,i,j} = \frac{G_{n,i,j+1} - G_{n,i,j}}{\Delta_S}, \qquad \mathrm{D}_S^- G_{n,i,j} = \frac{G_{n,i,j} - G_{n,i,j-1}}{\Delta_S},\\
&\mathrm{D}_{TT}^2 G_{n,i,j} = \frac{G_{n,i+1,j} - 2G_{n,i,j} + G_{n,i-1,j}}{\Delta_T^2}, \qquad \mathrm{D}_{SS}^2 G_{n,i,j} = \frac{G_{n,i,j+1} - 2G_{n,i,j} + G_{n,i,j-1}}{\Delta_S^2}\\
&\mathrm{D}_t^+ G_{n,i,j} = \frac{G_{n+1,i,j} - G_{n,i,j}}{\Delta_t}.
\end{aligned}$$

Substituting these expressions into the PDE above yields the following semi-linear equation for the grid point (t_n, m_i, τ_j)

$$\begin{aligned}
G_{n+1,i,j}\frac{1}{\Delta_t} = G_{n,i,j}\Big[&-M_1 + \frac{1}{\Delta_t} + \mathrm{abs}\Big(\frac{M_2}{\Delta_T}\Big) + \mathrm{abs}\Big(\frac{M_4}{\Delta_S}\Big) + 2\frac{M_3}{\Delta_T^2} + 2\frac{M_5}{\Delta_S^2}\Big]\\
&+ G_{n,i-1,j}\Big[\frac{M_2^-}{\Delta_T} - \frac{M_3}{\Delta_T^2}\Big] + G_{n,i+1,j}\Big[-\frac{M_2^+}{\Delta_T} - \frac{M_3}{\Delta_T^2}\Big]\\
&+ G_{n,i,j-1}\Big[\frac{M_4^-}{\Delta_S} - \frac{M_5}{\Delta_S^2}\Big] + G_{n,i,j+1}\Big[-\frac{M_4^+}{\Delta_S} - \frac{M_5}{\Delta_S^2}\Big]\\
&+ \delta\theta G_{n,i,j}^{1-1/\theta} c_{n,i,j}^{1-1/\psi}
\end{aligned}$$

Therefore, for a fixed point in time each grid point is determined by a non-linear equation. This results in a non-linear system of $(N_S+1)(N_T+1)$ equations that can be solved for the vector

$$G_n = (G_{n,1,1}, \cdots, G_{n,1,N_S}, G_{n,2,1}, \cdots, G_{n,2,N_S}, \cdots, G_{n,N_T,1}, \cdots, G_{n,N_T,N_S}).$$

Using this solution we update our conjecture for the optimal controls at the current point in the time dimension. We apply the first-order conditions and finite difference approximations of the corresponding derivatives. In the interior of the grid, we use centered finite differences. At the boundaries, we apply forward or backward differences.

C.2 Stochastic Discount Factor and Risk Premia

The dynamics of the SDF and the asset prices involve some yet unknown variables. For instance, the risk-free rate (6.3) involves the unknown drift and volatility vector of the consumption-capital ratio. These variables depend on the reduced-form value function G in (A.3) and its partial derivatives in a highly nonlinear manner. We thus calculate these variables numerically using finite differences. An application of Itôs lemma to $c = c(t,S,T)$ implies

$$\mathrm{d}c = c_t \mathrm{d}t + c_S \mathrm{d}S + c_T \mathrm{d}T + \frac{1}{2} c_{TT} \|\sigma_T\|^2 \mathrm{d}t + \frac{1}{2} c_{SS} \|\sigma_S\|^2 \mathrm{d}t$$

where

$$\mu_c(t,S,T) = \frac{1}{c}\big[c_t + c_S S(1-S)\mu_S + c_T \mu_T + \frac{1}{2} c_{TT} \|\sigma_T\|^2 + \frac{1}{2} c_{SS} S^2 (1-S)^2 \|\sigma_S\|^2\big], \tag{C.1}$$

$$\sigma_c(t,S,T) = \frac{1}{c}\big[c_S S(1-S)\sigma_S + c_T \sigma_T\big] \tag{C.2}$$

Since c is given by (A.2) and the optimal controls have already been calculated, we can use finite differences again to determine c and its partial derivatives. Then, we substitute them into (C.1) and (C.2) to obtain the relavant drift and volatility vector.

D Details of the Calibration

To calibrate the relevant parameters, we follow Pindyck and Wang (2013). Their model only involves a single capital stock and abstracts from climate change, but it can be nested in our two-sector model. The model is well-suited to explain *historical* asset returns, since dirty capital has dominated the world economy in the past, but the influence of climate change on asset markets is almost negligible. In the long run, there might be a transition from dirty to green capital. Yet, the current share of green capital is only about 6% indicating that the transition to green energy has been very modest.[22] We consider the special case of our model with only one capital stock and assume that it evolves as

$$\mathrm{d}K = \Big(I - \frac{1}{2}\phi \frac{I^2}{K} - \delta_k K\Big)\mathrm{d}t + K\sigma \mathrm{d}W_1 - K\ell_e \mathrm{d}N_e.$$

[22] See the website of the UNFCCC. https://unfccc.int/news/green-economy-overtaking-fossil-fuel-industry-ftse-russel-report

where output is given by $Y = AK^{1-\eta}F^{\eta} = I + C + \frac{b}{1+1/\varepsilon}F^{1+1/\varepsilon}K^{-1/\varepsilon}$. In the social optimum, the model collapses to a simple AK-technology with linear production function $Y = A^*K$ where productivity is

$$A^* = A\Big(\frac{b}{\eta A}\Big)^{\frac{\eta}{\eta-1-1/\varepsilon}} \tag{D.1}$$

The one-sector model is similar to that of Pindyck and Wang (2013), but involves an energy input F, which does not cause climate change. We fix the dividend leverage parameter at $\varphi = 2.8$ as it is common in the literature, e.g., Bansal and Yaron (2004). We choose a time preference rate of $\delta = 0.015$ per annum, which is standard in the literature on optimal carbon pricing, e.g., Nordhaus (2017). We follow van den Bremer and van der Ploeg (2021) and use energy shares of $\eta_i = 0.066$.

We calibrate the remaining parameters of this one sector model such that it generates a real expected growth rate of consumption of $\overline{\mu}_c = 2\%$, an average consumption rate of $\chi = \frac{C}{A^*K} = 75\%$ of GDP, a risk-free interest rate starting at $r^f = 0.8\%$, an average risk premium of $\text{rp} = 6.6\%$, and Tobin'Q's of $q = 1.58$. The following equations constitute a non-linear system that relates ψ, γ, A^*, ϕ, and φ to the quantities.

$$\chi = \frac{q}{A^*}\Big[\delta + \Big(\frac{1}{\psi} - 1\Big)\Big(\overline{\mu} - 0.5\gamma\sigma^2 - \frac{\lambda_d}{\alpha - \gamma + 1}\Big)\Big] \tag{D.2}$$

$$\overline{\mu}_c = -\delta_k + A\Big(1 - \chi - \frac{\eta}{1+1/\varepsilon}\Big) - \frac{1}{2}\phi A^2\Big(1 - \chi - \frac{\eta}{1+1/\varepsilon}\Big)^2 - \frac{\lambda_e}{\alpha_e + 1} \tag{D.3}$$

$$r^f = \delta + \frac{\overline{\mu}_c}{\psi} - \frac{1}{2}\gamma\Big(1 + \frac{1}{\psi}\Big)\sigma_c^2 - \lambda_e\frac{\Big(\frac{1}{\psi} - \gamma\Big)(\alpha_e - \gamma) + \gamma(\alpha_e - \gamma + 1)}{(\alpha_e - \gamma)(\alpha_e - \gamma + 1)} \tag{D.4}$$

$$\text{rp} = \varphi\gamma\sigma_c^2 + \lambda_e\gamma\Big[\frac{1}{\alpha_e - \gamma} - \frac{\alpha_e}{(\alpha_e + \varphi)(\alpha_e - \gamma + \varphi)}\Big] \tag{D.5}$$

$$q = \frac{1}{1 - \phi i} \tag{D.6}$$

For the derivation of these equations and for further details, we refer to Pindyck and Wang (2013). Finally, we back out the total factor productivity A from (D.1)

Next, we calibrate the cost parameters b_1 and b_2. Following van den Bremer and van der Ploeg (2021), we use energy shares $\eta_i = 0.066$ and use an average global cost of fossil fuel 540 USD per ton of carbon. We use a significantly higher average global price of green energy, i.e., 810 USD for the same amount of energy, which is in line with production costs in developed countries such as Germany. The optimal solution to this one-sector model implies that the aggregate costs of energy are given by

$$\frac{b}{1+1/\varepsilon}\Big(\frac{Y}{A^*}\Big)^{-1/\varepsilon}F^{1+1/\varepsilon} = \frac{\eta Y}{1+1/\varepsilon} \tag{D.7}$$

Given the average values $\overline{b}$, the optimal BAU-energy use must satisfy $F = \frac{\eta Y}{\overline{b}(1+1/\varepsilon)}$. Therefore, (D.7) determines the cost parameters b.

E State-Space Solutions

This appendix discusses the influence of the state variables on the optimal decisions and asset returns. From this, we derive intuition for the influence of the share of dirty capital and temperature on the optimal controls and understand the economic forces at play. In particular, we discuss how climate change affects the interest rate and asset returns. All the results are for the benchmark calibration for the year 2100 and for the level impact (L–I). The policy functions behave in a qualitatively similar manner for other years and for our alternative parametrizations of damages. The qualitative behavior of the asset returns is hardly affected by the choice of the damage specification. The lines in Figure E.1 present various levels of the capital share: The dark lines (——) depict $S = 0.9$, the gray lines (——) refers to $S = 0.5$, and the light lines (——) to $S = 0.1$. The horizontal axis depicts the temperature in the range from 0°C to 5°C.

Panel a) of Figure E.1 shows that the optimal investment in the green capital stock decreases in the share of dirty capital S, whereas Panel b) shows that the opposite is true for the investment in the dirty capital stock. This can be explained by the diversification argument from Section 3. If damages are moderate (as for the DICE damage specification), the economy retains a certain level of dirty capital to reach an optimal level of diversification. Therefore, the agent invests more in the green capital stock if the share of dirty capital is high and more in the dirty capital stock if this share is low. Panel c) shows that the optimal consumption strategy hardly depends on the share of dirty capital. This reflects the agent's motive for consumption smoothing. Instead of adjusting the consumption rate in response to the changes in the share of dirty capital, the economy increases the green investment ratio and decreases the dirty investment ratio to smooth consumption. Panel d) depicts fossil fuel use relative to the respective capital stock, which does not vary very much with the share of dirty capital. The corresponding ratio for green energy, F_1/K_1, does not depend on the share of dirty capital at all.[23] Panel e) depicts carbon emissions and shows that in absolute terms fossil fuel use decreases both in the share of dirty capital and temperature.

Panel f) depicts the optimal carbon tax as a fraction of total capital. It shows that the optimal carbon tax sharply increases in temperature and increases only moderately in the share of dirty assets. In recent years, a literature has evolved that derives simple formulas for the optimal social cost of carbon in deter-

[23] See the first-order condition (3.4).

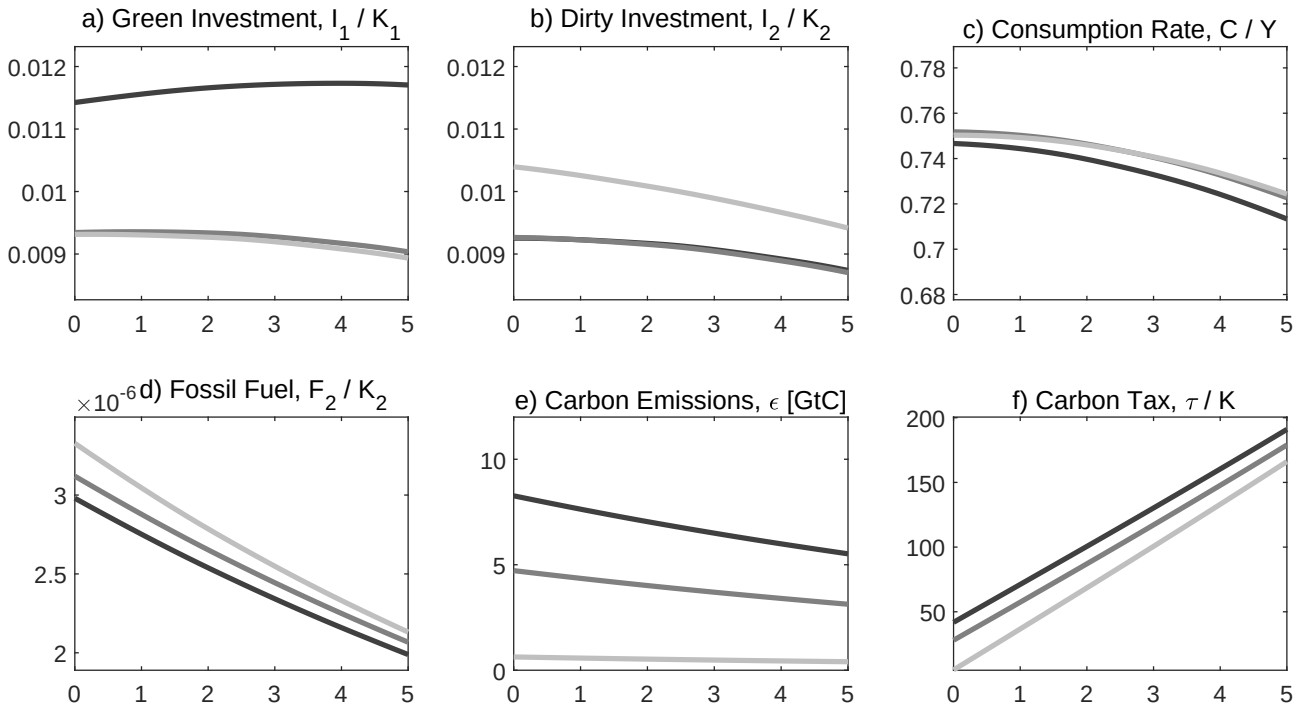

Figure E.1: Policy Functions with Level Impact. The graphs depict policy rules for the level impact as functions of the two state variables. On the horizontal axis is temperature in the range from 0°C to 5°C. The lines represent various levels of the capital share: dark lines (——) depict $S = 0.9$, gray lines (——) refer to $S = 0.5$, and light (——) lines to $S = 0.1$. a) plots green investment as a fraction of green capital, b) shows dirty investment as a fraction of dirty capital, c) depicts consumption as a fraction of output, d) shows green energy as a fraction of green capital, e) depicts fossil fuel use as a fraction of dirty capital, and f) shows the optimal carbon tax as a fraction of total capital.

ministic environments (e.g., Nordhaus 1991; Golosov et al. 2014, Rezai and van der Ploeg 2016; van den Bijgaart et al. 2016; van der Ploeg and Rezai 2019 and Hambel et al. 2021b). This strand of literature considers analytical models and generates social costs of carbon that do not depend on temperature.[24] By contrast, our framework explicitly models stochastic climate risks and uses a convex damage function, which yields temperature-dependent carbon taxes and optimal controls. Consequently, society reacts to increasing climate risks by raising carbon taxes and thus to more pronounced carbon abatement for higher temperatures. For the damage specification (D–I), damages are linear in temperature

[24]The reason is that the concavity of the logarithmic Arrhenius' law linking temperature to the atmospheric stock of carbon is (more or less) exactly offset by the convexity of the function relating the damage ratio to temperature (Golosov et al. 2014). For more convex damage ratios, the ratio of the optimal SCC to GDP increases in temperature (e.g., Rezai and van der Ploeg 2016).

rather than convex. In turn, the policy functions are almost independent of temperature as in the above mentioned strand of literature.[25]

F Optimal Policy Simulations

Here we present our our optimal policy simulation results over the next 100 years. The columns of Figures E.1 and F.2 show results for the two damage specifications (L–I), and (D–I), respectively. Unless otherwise stated, we use the benchmark calibration summarized in Table 1. Optimal paths are depicted by solid lines (——) and BAU paths by dotted lines (·····). Dashed lines (- - -) show 5% and 95% quantiles of the optimal solution. Appendix E shows the state-space solutions that are used to get these simulations.

F.1 Effects of Climate Policy on the Economy

Figure E.1 depicts the optimal evolution of the real economy under two different damage specifications. It shows that the qualitative behavior is similar for all specifications.

Panels a1)-a2) depict the time paths of output. As a result of climate action, the optimal evolutions exhibit a higher economic growth compared to the BAU evolution since some of the climate damages are avoided. This is true for both damage specifications. For the disaster impact, the climate damages are more pronounced and economic growth is significantly dampened compared to the level impact.

Panels b1)-b2) depict that the consumption-output ratio is in a narrow range between 74% to 77%. In particular, for the BAU case, the optimal consumption-output ratio sharply increases for high temperatures around 4°C. A potential explanation is the convexity of the damage function, which leads to a higher sensitivity to atmospheric temperature. For the other damage specification, which is linear in temperature, optimal consumption exhibit small variation across states. In the BAU case, optimal consumption is almost constant.

Panels c1)-c2) depict the evolution of the carbon dioxide emissions that are significantly dampened compared to the BAU case. In general, the variation of optimal emissions is low. As discussed in the previous section, optimal emissions are mainly driven by the share of dirty capital, while the influence of temperature is relatively weak. The small variation of the optimal carbon dioxide emissions thus follows from the small variation in S depicted in Panels d1)-d2). The evolution of the share of dirty capital is crucial for understanding the interaction between the diversification and the abatement motive. If we disregard damages from climate change, the share of dirty assets eventually stabilizes at $S^* = 50\%$. On

[25] The corresponding figures are available upon request.

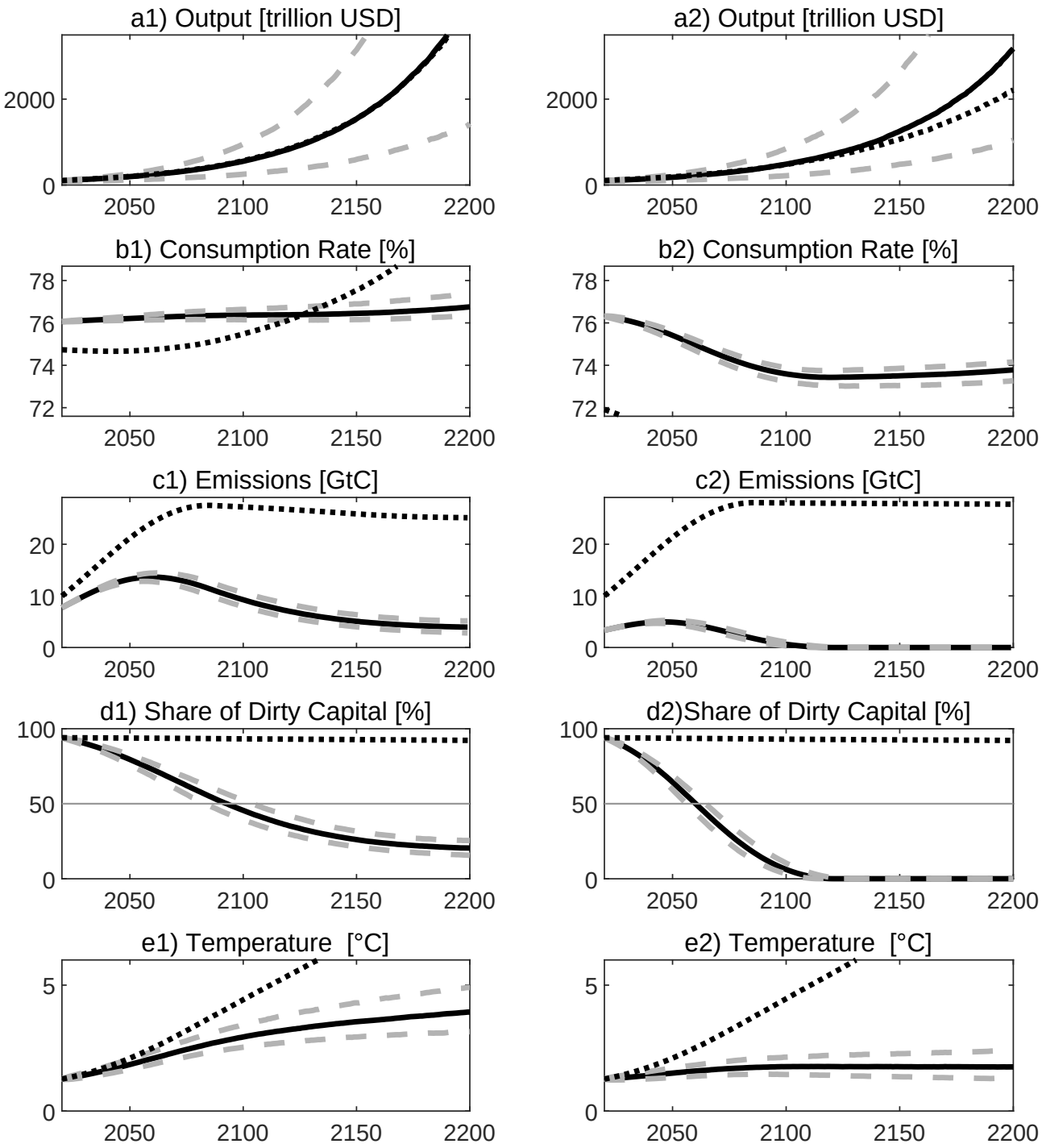

Figure E.1: Evolution of Temperature, the Social Cost of Carbon and the Real Economy. The figure depicts the simulation of the real economy for the two damage specifications level impact (1st column) and disaster impact (2nd column) until the year 2200. Median optimal paths are depicted by solid lines (——) and median BAU paths by dotted lines (·····). Dashed lines (- - -) show 5% and 95% quantiles of the optimal solution. Panels a1)-a2) show the evolution of output. Panels b1)-b2) depict the consumption rate expressed as a fraction of output, i.e., C/Y. Panels c1)-c2) depict the evolution of carbon emissions. Panels d1)-d2) show the evolution of the share of dirty capital S. Panels e1)-e2) depict the evolution of global average temperature increase and Panels f1)-f2) show the optimal carbon tax.

the other hand, if society recognizes climate change and fights global warming, the share of dirty capital decreases to approximately 20%. However, dirty capital does not vanish completely since some positive amount is kept to satisfy the diversification motive. In this sense, the diversification motive eventually reduces climate action.

F.2 Effects of Climate Policy on Asset Prices

Figure F.2 complements the results presented in Figure E.1 with asset pricing results. Panels a1)-a2) depict the evolution of the green Tobin's Q, whereas Panels b1)-b2) show the evolution of the dirty one. In the optimum, the green Tobin's Q decreases over time, but the dirty Tobin's Q remains always smaller than the green Tobin's Q. For the disaster impact, the green Q stabilize around 1.5, while for the level impact the green Tobin's Q continues to decrease below that level.

Panels c1)-c2) show that the equilibrium risk-free interest rate decreases for all scenarios including BAU, since over time the expected damages from global warming become more pronounced and households respond with higher precautionary savings. This effect is much stronger under BAU, since then climate damages are more severe. In contrast, if carbon is optimally priced, the downward trend of the risk-free interest rate is less pronounced.

Panels d1)-d2) show the evolution of the green risk premium, whereas Panels e1)-e2) depicts the evolution of the dirty risk premium. As discussed in the main text, the dirty risk premium depends on the state variables S and T in a non-linear way. This might explain the "snake-shaped" evolution of the dirty risk premium over time. For the disaster impact, the risk premiums are higher. This is triggered by the additional Poisson shock N_e which gives rise to an extra component in the risk premium, as seen in Proposition 6.1. Since the jump intensity increases in temperature and global warming becomes more significant over time, the relative importance of the extra component increases under BAU. This reflects the fact that asset holders must be compensated for the increasing climate risks.

G Robustness

G.1 Non-perfect Substitutes

We now consider two alternative model extensions that relax the assumption of perfectly substitutable final goods. (i) We assume that the consumption goods produced in both sectors are non-perfect substitutes and the agent gains utility from a CES consumption bundle $C = \left(C_1^\rho + C_2^\rho\right)^{\frac{1}{\rho}}$, where ρ is a constant and $\zeta = \frac{1}{1-\rho}$ denotes the elasticity of substitution. (ii) We also study an extension in the spirit of Ace-

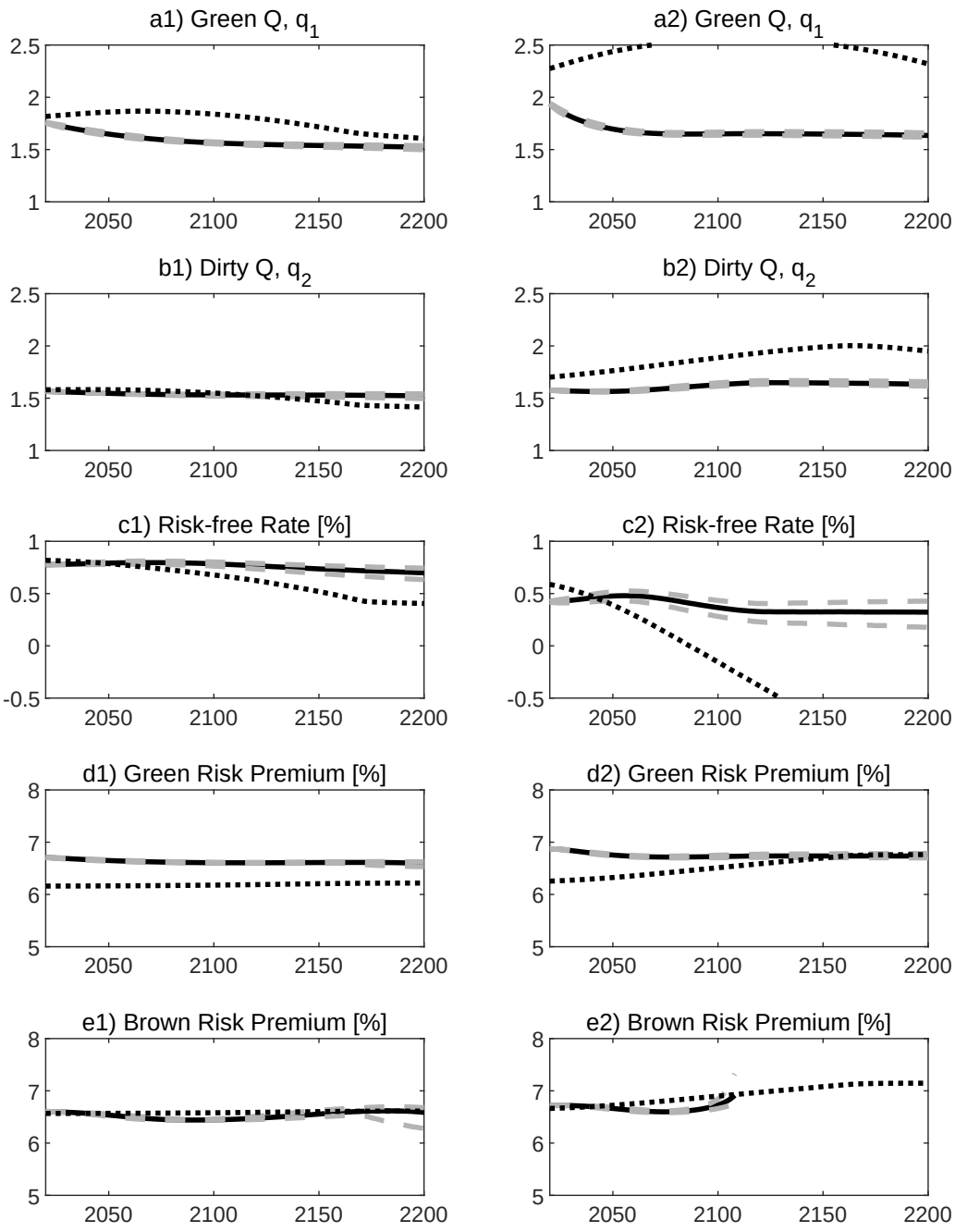

Figure F.2: Evolution of Tobin's Q's, Risk-Free Rates and the Risk Premiums. The figure depicts the simulation of the asset pricing quantities for the two damage specifications level impact (1st column) and disaster impact (2nd column) until the year 2200. Median optimal paths are depicted by solid lines (——) and median BAU paths by dotted lines (·····). Dashed lines (- - -) show 5% and 95% quantiles of the optimal solution. Panels a1)-a2) show the evolution of the Tobin's Q of the green asset and Panels b1)-b2) depict the evolution of the Tobin's Q of the dirty asset. Panels c1)-c2) depict the evolution of the equilibrium risk-free rate. Panels d1)-d2) show the evolution of the risk premium of the green asset. Panels e1)-e2) depict the evolution of the risk premium of the dirty asset.

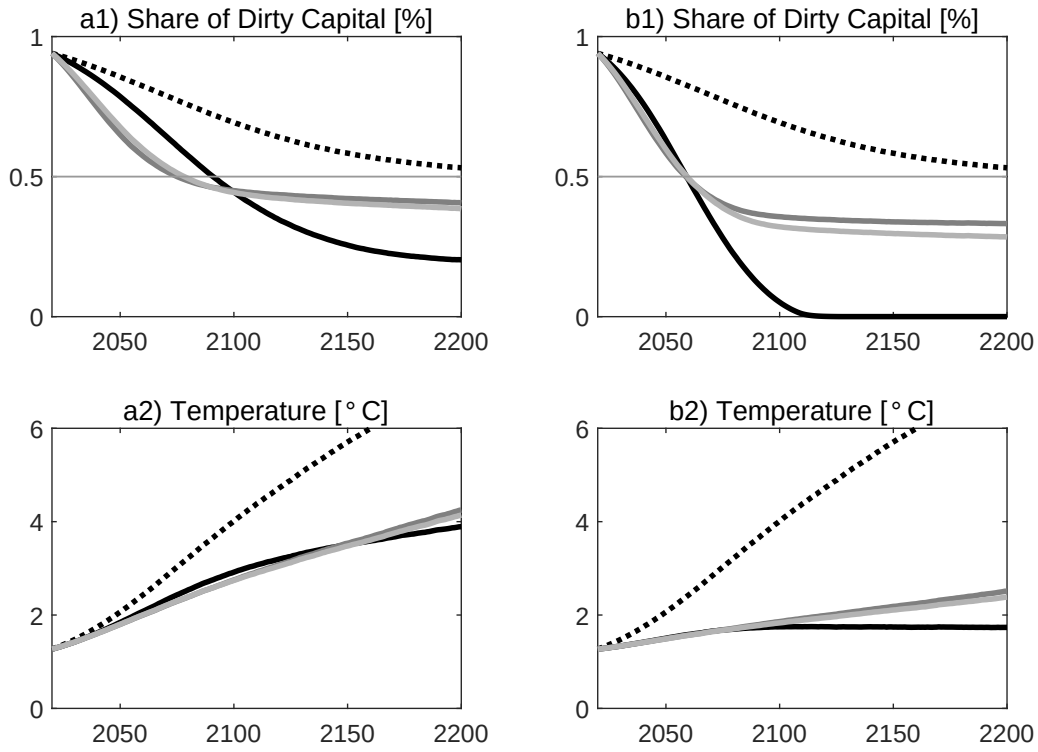

Figure G.1: Imperfect Substitutes. The figure depicts the simulation of the share of dirty capital and global average temperature for the two damage specifications level impact (1st column) and disaster impact (2nd column) until the year 2200. The black dotted lines (⋯⋯) show the results for a hypothetical scenario without damages from climate change. The black solid lines (——) show the results for benchmark setting with perfect substitutes. The gray lines (——) show results for imperfect substitutes in consumption ($\rho = 0.9$). The light lines (——) show results for imperfect substitutes in production ($\rho = 0.9$).

moglu et al. (2012) and assume that Y_1 and Y_2 are intermediate goods that must be aggregated to a final good via $Y = \left(Y_1^{\rho} + Y_2^{\rho}\right)^{\frac{1}{\rho}}$. Both extensions lead to significantly more involved first-order conditions and the solution requires additional computational costs. Separation theorems in the spirit of Proposition A.1 are available upon request.

Figure G.1 depicts the results for both model extensions each with $\rho = 0.9$ corresponding to an elasticity of substitution between the two sectors of $\zeta = 10$. The light lines (⋯⋯, ——) depict the results for imperfect substitutes in consumption (i), while the gray lines (⋯⋯, ——) in Figure G.1 show the results for imperfect substitutes in production (ii). The black lines (⋯⋯, ——) show the results for the benchmark case with perfect substitutes. In line with Acemoglu et al. (2012), we find that a higher elasticity of substitution leads to more and faster abatement. A lower elasticity between the two sectors significantly increases the demand for dirty goods in order to sustain production. Hence, additionally to the

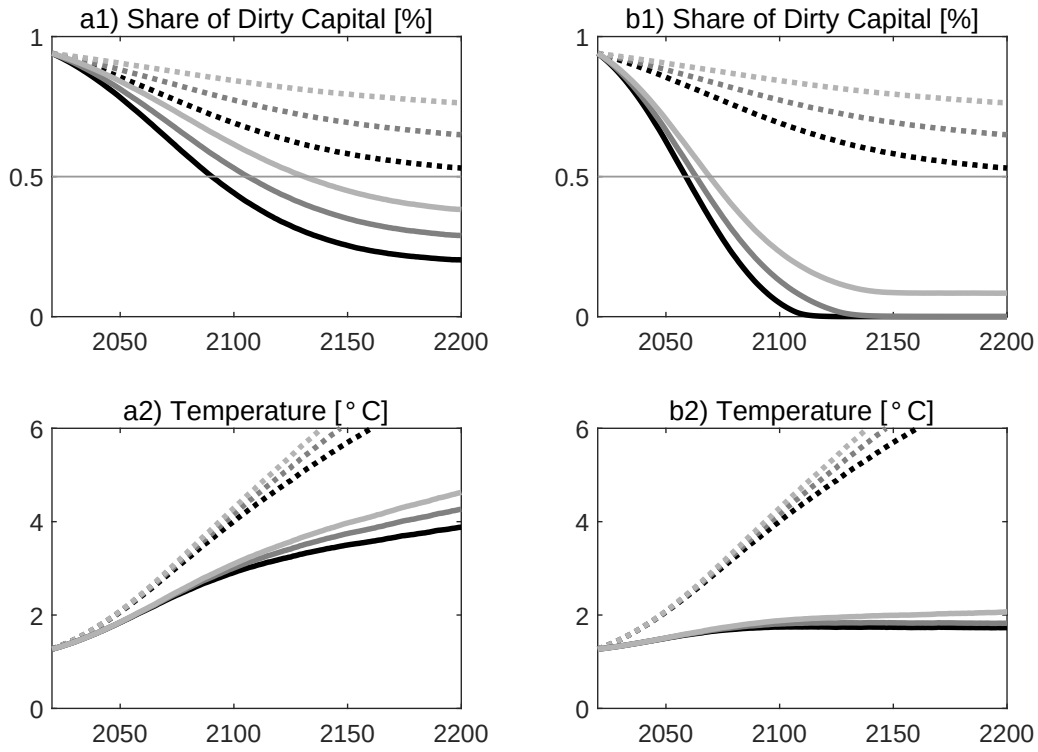

Figure G.2: Varying Total Factor Productivity. The figure depicts the simulation of the share of dirty capital and global average temperature for the two damage specifications level impact (1st column) and disaster impact (2nd column) until the year 2200. The black dotted lines (·····) show the results for a hypothetical scenario without damages from climate change. The black solid lines (——) show the results for the benchmark values of total factor productivity $A_1 = 0.1058$, $A_2 = 0.1030$, or equivalently $A_1^* = A_2^* = 0.0449$. The gray lines (——) show results with a lower productivity of the green sector of $A_1 = 0.1044$, or equivalently $A_1^* = 0.0442$, i.e., about 1.5% smaller than the carbon-intensive sector. The light lines (——) show results for when $A_1 = 0.1030$, or equivalently $A_1^* = 0.0436$, i.e., about 3% smaller than the carbon-intensive sector.

abatement motive and the financial diversification motive, a third effect materializes, which is due to the desire to diversify the production process (i) or the consumption bundle (ii), respectively. In either case, this effect hampers the transition towards a low-carbon economy.

G.2 Asymmetric Calibration

This section analyzes the influence of an asymmetric calibration of the effective total factor productivity. In the benchmark calibration both sectors are assumed to be equally productive with $A_1^* = A_2^* = 0.0449$. Now we assume that the different costs of energy across the two sectors lead to different effective productivities and, in turn, the green sector generates slightly lower economic growth rates compared to the benchmark case. The black lines (·····, ——) in Figure G.2 show the results for the benchmark

Impact	Benchmark (——)	Double Impact (——)	Triple Impact (——)
Level	$\theta_i = 0.00236$	$\theta_i = 0.00472$	$\theta_i = 0.00708$
Disaster	$\lambda_c(T) = 0.003 + 0.096T$	$\lambda_c(T) = 0.003 + 0.192T$	$\lambda_c(T) = 0.003 + 0.288T$

Table G.1: Different Intensities for the Specifications of Global Warming Damages. The table summarizes the different damage specifications that are used in Figure G.3.

case. The gray lines (·····, ——) show the results for when the effective productivity of the green sector is about 1.5% smaller than the carbon-intensive sector. The light lines (·····, ——) depict the results for when the effective productivity of the green sector is about 3% smaller than the carbon-intensive sector. It turns out that lowering the productivity of the green sector in response to higher energy costs hampers the transition towards a low-carbon economy and the planner wants to keep a larger share of dirty capital alive. Hence, as for asymmetric volatility parameters, the share of dirty capital stabilizes at a level different from 50%.

G.3 Effects of Different Damage Specifications

Figure G.3 depicts the influence of the damage specification on the optimal evolution of the share of dirty capital and global temperature. The black dotted lines (·····) show the results for a hypothetical scenario where climate change does not generate economic damages, in which case only the diversification motive matters. If economic damages from climate change are pronounced, the abatement motive comes into play and the optimal level of the share of dirty capital shifts down to a social optimum below $S = 50\%$. The black solid lines (——) show the results for the damage parameters presented in Section 4. The gray lines (——) depict results with damage parameters that are twice as high. The light lines (——) show results with damage parameters that are three times higher. Table G.1 summarizes the damage parameters that are used in Figure G.3. It can be seen that for higher damage parameters the abatement motive becomes more pronounced and the diversification motive loses its importance. For sufficiently high damages, the dirty capital stock vanishes and production of carbon-intensive goods ceases. This increases the volatility of total capital, but the benefits from abatement eventually dominate the benefits from diversification. Doubling or tripling the damage parameter for the disaster impact has only a moderate influence since the benchmark calibration is already severe enough to bring the share of dirty capital to zero. The effect for the level impact is more pronounced.

Figure G.4 studies the effect of a simultaneous level and disaster impact (——). Since the disaster impact (——) is much more pronounced than Nordhaus' level impact (——), the latter is dominated by

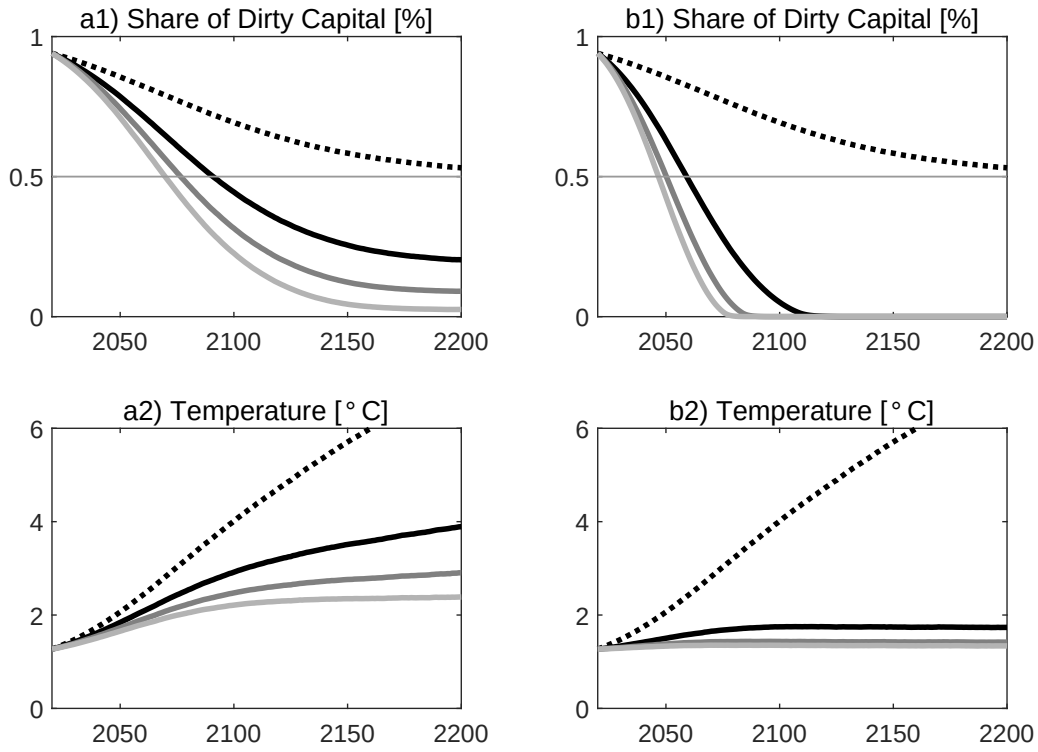

Figure G.3: Increasing Intensities of Global Warming Damages. The figure depicts the simulation of the share of dirty capital and global average temperature for the two damage specifications level impact (1st column) and disaster impact (2nd column) until the year 2200. The black dotted lines (⋯⋯) show the results for a hypothetical scenario without damages from climate change. The black solid lines (——) show the results for the damage parameters as calibrated in Section 4. The gray lines (——) show results with damage parameters that are twice as high as in the benchmark calibration. The light lines (——) show results with damage parameters that are three times higher than those from the benchmark calibration. The main insight from this figure is that with higher intensities of damages than our benchmark damages, the abatement motives becomes relatively more important than the diversification motive and leads to a lower or even a zero dirty capital stock in the long run.

the disaster impact. Hence, switching on the level impact does not lead to significantly more abatement, nor signifacantly higher carbon taxes (not shown in the figure).

G.4 Reallocation Costs

This section analyzes the influence of the reallocation cost parameter κ on the interplay between diversification and climate action. Figure G.1 depicts the results. The light lines (⋯⋯, ——) depict the results for high reallocation costs, $\kappa = 5$, the gray lines (⋯⋯, ——) show the results for a low reallocation cost parameter, $\kappa = 0.5$. The black lines (⋯⋯, ——) show the results for the benchmark case with $\kappa = 2$. A

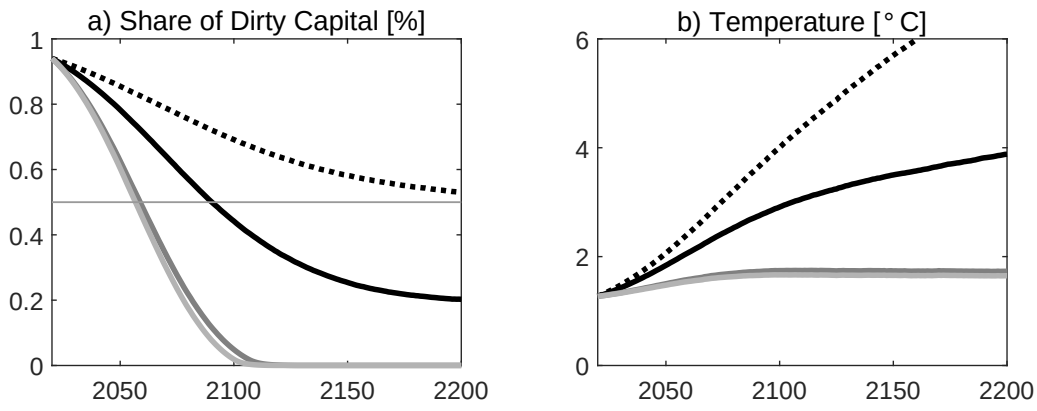

Figure G.4: Damage Specification. The figure depicts the simulation of the share of dirty capital and global average temperature for the damage specifications level impact (——), disaster impact (——), and simultaneous level and disaster impact (——) until the year 2200. The black dotted lines (·····) show the results for a hypothetical scenario without damages from climate change.

higher value of κ leads to more sticky investment decisions as the reallocation of dirty capital into green capital is more expensive. Figure G.5 shows that on the long run the optimal share of dirty capital in the economy is independent of this parameter indicating that κ only influences the speed of the transition, but not the level of stabilization.

G.5 Different Instantaneous Volatilities

This section complements Section 5.3, which studies the influence of asymmetric instantaneous volatilities. Now, we study the effect of symmetric volatilities that differ from our benchmark calibration. Figure G.6 depicts the results. The black lines (·····, ——) show the results for the benchmark case with $\sigma_n = 2\%$. The light lines (·····, ——) depict the results for higher volatility, $\sigma_n = 3\%$, and the gray lines (·····, ——) show the results for lower volatility, $\sigma_n = 1\%$. The figure shows that lower volatility decreases the importance of the diversification motive and thus society keeps less carbon-intensive capital in the economy. In the limiting case of $\sigma_n = 0$ both capital stocks would be perfectly correlated to each other, and thus the carbon-intensive capital stock would eventually be run down.

G.6 Different Instantaneous Correlations

Correlations play a crucial role for diversification. Figure G.7 depicts the optimal evolution of the share of dirty capital for for different values of the instantaneous correlation ρ_{12} and for the two damage specifications, level impact (1st column) and disaster impact (2nd column). Black lines (·····,——) show

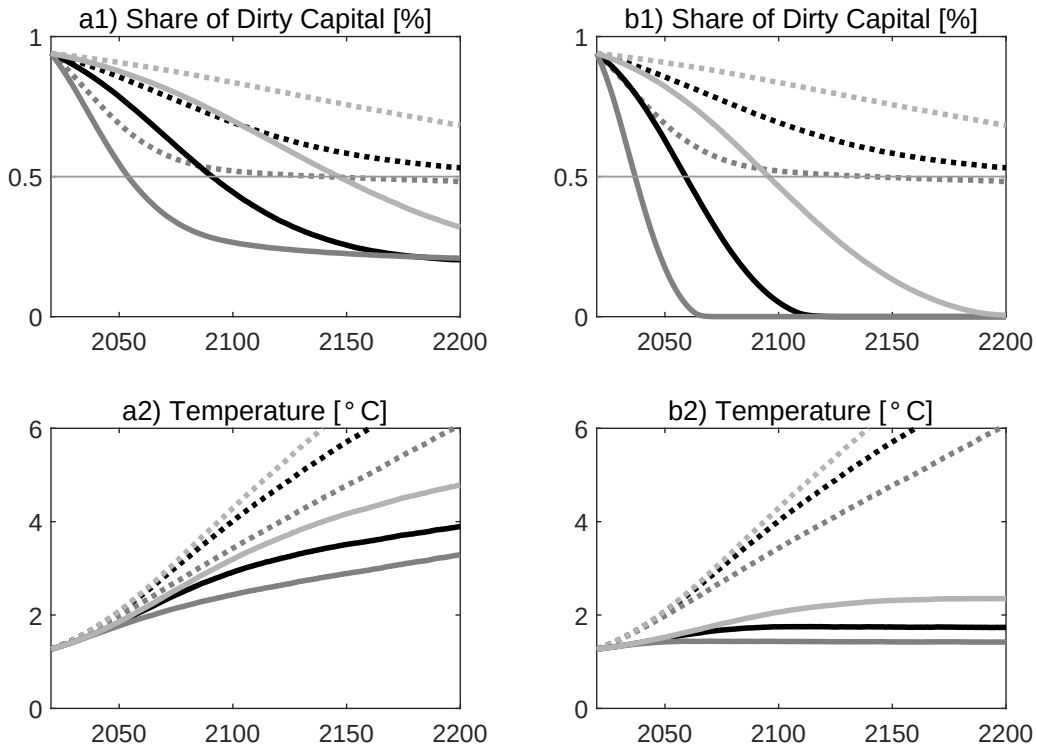

Figure G.5: Reallocation Cost Parameter. The figure depicts the simulation of the share of dirty capital and global average temperature for the two damage specifications level impact (1st column) and disaster impact (2nd column) until the year 2200. The dotted lines (⋯⋯) show the results for a hypothetical scenario without damages from climate change. The black solid lines (——) show the results for a benchmark cost parameter of $\kappa = 2$. The gray lines (——) show results with a low reallocation cost parameter $\kappa = 0.5$. The light lines (——) show results for when reallocation is more expensive $\kappa = 5$.

results for the benchmark case $\rho_{12} = 0$. Gray lines (⋯⋯, ——) show results for $\rho_{12} = -0.5$. Light lines (⋯⋯, ——) depict results for $\rho_{12} = 0.5$. Dotted lines depict results for hypothetical scenarios without damages from climate change.

A negative correlation coefficient (⋯⋯, ——) amplifies the diversification motive. This leads to a faster transition to full diversification of $S = 50\%$. In the short run, this effect accelerates decarbonization of the economy, but in the long run the opposite is true, see Panels a1)-a2) of Figure G.7. The economy keeps a higher share of dirty capital to benefit from diversification even in case of the disaster impact. In turn, the transition is slowed down and the share of dirty capital stabilizes at a higher level compared to the case with zero correlation. In other words, there is less climate action in the long run if the benefits from diversification are more pronounced.

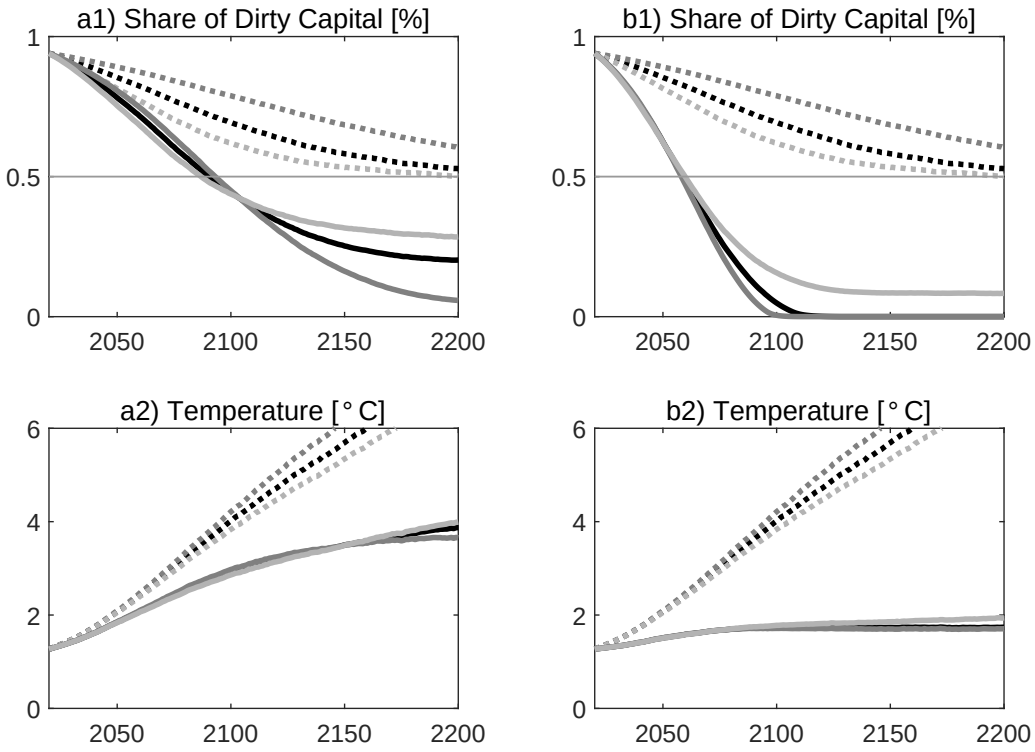

Figure G.6: Different Instantaneous Volatilities. Solid lines depict the optimal evolution of the share of dirty capital and global average temperature for the two damage specifications level impact (1st column) and disaster impact (2nd column) until the year 2200. Dotted lines show the results for hypothetical scenarios without damages from climate change. Black lines (⋯⋯, ——) show results for the benchmark case where $\sigma_n = 2\%$. Gray lines (⋯⋯, ——) show results for a lower volatility of shocks to the dirty sector, $\sigma_n = 1\%$. Light lines (⋯⋯, ——) depict the results for a higher volatility of shocks to the dirty sector, $\sigma_n = 3\%$.

For a positive correlation coefficient, the diversification motive is less important, which can be seen from the gray dotted lines (⋯⋯). In the short run, transition from a carbon-intensive to a carbon-free economy is significantly slowed down. In the long run, however, the abatement motive dominates and the share of dirty assets stabilizes at lower levels (——). Hence, the speed of decarbonization is significantly effected by the sign and size of the correlation coefficient between the green and dirty capital stock.

While S denotes the share of dirty capital, we are also interested in the share π of dirty assets in the world portfolio held by the representative investor, i.e.,

$$\pi = \frac{P_2}{P_1 + P_2} \tag{G.1}$$

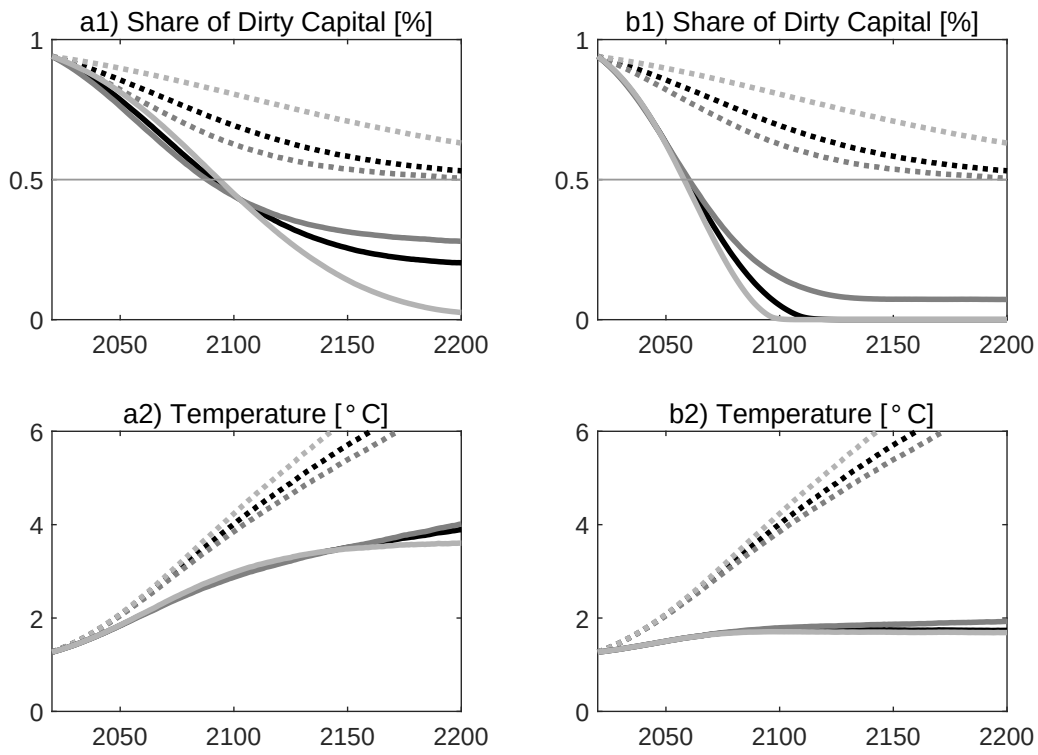

Figure G.7: Different Instantaneous Correlations. Solid lines depict the optimal evolution of the share of dirty capital and global average temperature for the two damage specifications level impact (1st column) and disaster impact (2nd column) until the year 2200. Black lines (⋯⋯, ——) show results for the benchmark case where the correlation between the Brownian shocks affecting the green and dirty sector is $\rho_{12} = 0$. Gray lines (⋯⋯, ——) show results with $\rho_{12} = -0.5$. Light lines (⋯⋯, ——) depict the results with $\rho_{12} = 0.5$. Dotted lines show the corresponding results for hypothetical scenarios without damages from climate change.

Figure G.8 depicts the analogous results for the share of dirty asset instead of the share of dirty capital. We find that the results are qualitatively similar although the asset shares stabilize at lower levels than the capital shares. This can be explained by the fact that the green asset has lower dividend yields than the carbon-intensive asset, hence the green asset prices grow faster than the dirty asset prices (see Table 3) and the denominator in (G.1) eventually becomes relatively larger than the denominator in the definition of S.

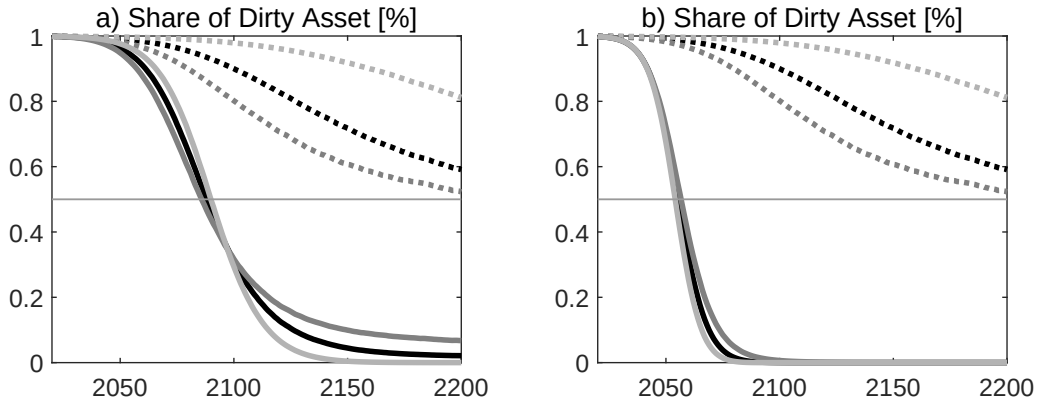

Figure G.8: Share of Asset Prices for Different Instantaneous Correlations. Solid lines depict the optimal evolution of the share of dirty asset $\pi = P_2/(P_1 + P_2)$ for the two damage specifications level impact (1^{st} column) and disaster impact (2^{nd} column) until the year 2200. Black lines (⋯⋯ ,——) show results for the benchmark case where the correlation between the Brownian shocks affecting the green and dirty sector is $\rho_{12} = 0$. Gray lines (⋯⋯ , ——) show results with $\rho_{12} = -0.5$. Light lines (⋯⋯ , ——) depict the results with $\rho_{12} = 0.5$. Dotted lines show the corresponding results for hypothetical scenarios without damages from climate change.